CFTR: Covalent and Noncovalent Modification Suggests a Role for Fixed Charges in Anion Conduction

Stephen S. Smith,[1,2] Xuehong Liu,[1,2] Zhi-Ren Zhang,[3,4] Fang Sun,[2] Thomas E. Kriewall,[2] Nael A. McCarty,[3,4] and David C. Dawson[1,2]

[1]Department of Physiology and Pharmacology, Oregon Health Sciences University, Portland, OR 97201
[2]Department of Physiology, University of Michigan, Ann Arbor, MI 48109
[3]Department of Physiology, and [4]Center for Cell and Molecular Signaling, Emory University, Atlanta, GA 30322

ABSTRACT The goal of the experiments described here was to explore the possible role of fixed charges in determining the conduction properties of CFTR. We focused on transmembrane segment 6 (TM6) which contains four basic residues (R334, K335, R347, and R352) that would be predicted, on the basis of their positions in the primary structure, to span TM6 from near the extracellular (R334, K335) to near the intracellular (R347, R352) end. Cysteines substituted at positions 334 and 335 were readily accessible to thiol reagents, whereas those at positions 347 and 352 were either not accessible or lacked significant functional consequences when modified. The charge at positions 334 and 335 was an important determinant of CFTR channel function. Charge changes at position 334—brought about by covalent modification of engineered cysteine residues, pH titration of cysteine and histidine residues, and amino acid substitution—produced similar effects on macroscopic conductance and the shape of the I-V plot. The effect of charge changes at position 334 on conduction properties could be described by electrodiffusion or rate-theory models in which the charge on this residue lies in an external vestibule of the pore where it functions to increase the concentration of Cl adjacent to the rate-limiting portion of the conduction path. Covalent modification of R334C CFTR increased single-channel conductance determined in detached patches, but did not alter open probability. The results are consistent with the hypothesis that in wild-type CFTR, R334 occupies a position where its charge can influence the distribution of anions near the mouth of the pore.

KEY WORDS: thiol reagents • anion channel • *Xenopus* oocytes • surface charge • cystic fibrosis

INTRODUCTION

The proposed topology of the CFTR includes 12 transmembrane spanning segments (TMs),* and it is generally agreed that some or all of these must contribute to the formation of an anion-selective pore (Riordan et al., 1989; Dawson et al., 1999; McCarty, 2000). Mutations in the TMs influence the conduction properties of CFTR (Anderson et al., 1991; Tabcharani et al., 1993; McDonough et al., 1994; Linsdell et al., 1998, 2000; Mansoura et al., 1998; Guinamard and Akabas, 1999; Zhang et al., 2000a,b; McCarty and Zhang, 2001), and cysteines substituted into some of the TMs have been reported to be accessible to externally applied thiol reagents (Akabas et al., 1994; Cheung and Akabas, 1996; Akabas, 1998), but the molecular determinants of anion conduction have not been identified.

We recently proposed that the lyotropic anion selectivity sequence that is characteristic of CFTR could be explained by a relatively simple model that envisions the pore as a dielectric tunnel into which halides and pseudohalides partition from water, as expected from their effective radii. This model provides a physical interpretation of relative anion permeability and relative anion binding, but does not address the molecular basis of pore conductance. Herein, we present evidence that one of the important determinants of pore conductance is charged residues that reside in or near the pore.

We chose transmembrane segment 6 (TM6) for initial study because it has been implicated by a number of laboratories (Anderson et al., 1991; Sheppard et al., 1993; Tabcharani et al., 1993; McDonough et al., 1994; Mansoura et al., 1998) as being a critical determinant of CFTR conduction properties, and because it contains four basic residues that span TM6 from the predicted extracellular end (R334 and K335) to the predicted cytoplasmic end (R347 and R352), so that based on the electrostatic considerations alone, it seemed likely to play an important role in anion conduction. The experimental strategy was based on comparison of

S.S. Smith and X. Liu made equal contributions to this work.

Address correspondence to David C. Dawson, Department of Physiology and Pharmacology, L334, 3181 SW Sam Jackson Park Road, Portland, OR 97201. Fax: (503) 494-4352; E-mail: dawsonda@ohsu.edu

*Abbreviations used in this paper: IBMX, 3-isobutyl-methylxanthine; 2-ME, 2-mercaptoethanol; MTSEA, 2-(aminoethyl) methanethiosulfonate; MTSES, 2-sulfonatoethyl methanethiosulfonate; MTSET, [2-(trimethylammonium)ethyl] methanethiosulfonate; NEM, *N*-ethylmaleimide; P_o, open probability; RR, rectification ratio; TM, transmembrane spanning segment; wt CFTR, wild-type CFTR.

the conduction properties of CFTR constructs in which charges were modified using covalent modification of engineered cysteine residues, pH titration of engineered cysteine or histidine residues, and conventional site-directed mutagenesis. In some cases, the results that we obtained with covalent modification techniques differed from those previously reported (Cheung and Akabas, 1996; Cheung and Akabas, 1997) so we endeavored to validate the effects of covalent modification by comparison to other methods. The results are consistent with a model that assigns to R334 a critical role in the determination of CFTR pore conductance that derives, at least in part, from the influence of its positive charge on the distribution of anions adjacent to the mouth of the pore.

MATERIALS AND METHODS

Site-directed Mutagenesis, RNA Synthesis and Xenopus Oocyte Expression

Site-directed mutations were engineered using a nested PCR strategy in which the mutation was designed into antiparallel oligomers that were first round-amplified along with flanking oligomers (at AflII and SphI, respectively). Second round amplification was done using the flanking oligomers alone. The AflII-SphI fragment was subcloned back into a pBluescript vector (pBQ4.7; Drumm et al., 1991) containing human wild-type CFTR (wt CFTR) from which the native AflII-SphI fragment had been separated. All mutations were confirmed by direct sequencing of the entire fragment before subcloning. R347C and R352C were gifts of M. Akabas (Albert Einstein College of Medicine, Bronx, NY) and used in their parent vector, pMN. These constructs were sequenced to confirm the point mutations. A number of the constructs were expressed in both vectors to ensure that there were no differences between the two. The pMN vector yields slightly higher expression levels than the pBQ4.7 vector. For the purpose of evaluating the effect of modifying reagents independently of CFTR expression, we used a cysteine-substituted potassium channel, Kv2.1 (I379C), which was provided by R. Joho (University of Texas Southwestern Medical Center, Dallas, TX; Zhang et al., 1996). To evaluate nonspecific effects that may be due to the stimulating cocktail, we coexpressed CFTR with the β-adrenergic receptor and stimulated with isoproterenol (McCarty et al., 1993). The β-adrenergic receptor was a gift of H. Lester (California Institute of Technology, Pasadena, CA). The vector containing wt CFTR or the variants was linearized with XhoI (pBQ4.7) or SmaI (pMN), Kv2.1(I379C) was linearized with NotI, and the β-adrenergic receptor was linearized with HindIII. The linearized plasmid was used as template for the generation of cRNA using the mMessage mMachine protocol (Ambion). The cRNA was resuspended in diethyl pyrocarbonate–treated water and maintained at −70°C before injection into oocytes.

The methods for oocyte harvesting have been extensively documented (Goldin, 1992; Wilkinson et al., 1996). In brief, female *Xenopus* (*Xenopus*-1) were anesthetized by immersion in ice water containing 3-aminobenzoic acid ethyl ester (tricaine, 3 mg/ml; Sigma-Aldrich), and oocytes were removed through an abdominal incision. The follicular membrane was removed by mechanical agitation (2–3 h) in a nominally Ca^{2+}-free, collagenase solution containing the following (in mM): 82.5 NaCl, 2 KCl, 1 $MgCl_2$, 10 HEPES, pH 7.5, and 2.5 mg/ml collagenase (GIBCO BRL). Defolliculated oocytes were maintained in a modified Barth's solution (MBSH) containing the following (in mM): 88 NaCl, 1 KCl, 2.4 $NaHCO_3$, 0.82 $MgSO_4$, 0.33 $Ca(NO_3)_2$, 0.41 $CaCl_2$, 10 HEPES, pH 7.5, and 150 mg/liter gentamicin sulfate. Oocytes were maintained at 18°C in a humidified incubator. On the day after isolation, oocytes were injected with cRNA (diluted in diethyl pyrocarbonate–treated water to give 50–250 μS of stimulated conductance (~0.15 ng/oocyte for most constructs, but 5–10 ng/oocyte for R352 variants). In each case, a 50-nl volume was injected into each oocyte using a microinjector (Drummond) and beveled injection needles (~10-μm tip diameter). Injected oocytes were maintained in MBSH, and used for electrophysiological analysis 2–6 d after injection.

Electrophysiology

Individual oocytes were continuously perfused (4 ml/min) at room temperature with an amphibian Ringer's solution containing the following (in mM): 98 NaCl, 2 KCl, 1.8 $CaCl_2$, 1 $MgCl_2$, and 5 HEPES, pH 7.5. For those experiments in which the bath pH was modified, HEPES was replaced with either MES (for pH 6.5 or less) or TAPS (pH 8 or greater). The different buffers produced no discernible differences in the electrical behavior of wt CFTR. Oocytes were impaled with two microelectrodes with tips pulled (Sutter Instrument Co.) to yield a resistance of 0.5–1.5 MΩ when filled with 3 M KCl. Two reference electrodes were used in a current monitor/bath clamp configuration so that the bath was always clamped to 0 mV (model TEV 200; Dagan Corp.). The open circuit membrane potential was continuously monitored on a strip chart recorder (Kipp and Zonen), and periodically V_m was clamped and, using a computer driven protocol (pClamp; Axon Instruments, Inc.), ramped from −120 to +60 mV at a rate of 100 mV/s for most analyses. For ramp data, a correction for the capacitive current was estimated by comparing the current at the holding potential to the same potential within the ramp, and the difference was subtracted from the entire event. A step protocol (from −120 to +60 mV in 20-mV steps, 200–500 ms/step) was also used to check for time-dependent currents. The membrane conductance was calculated from either the slope conductance over a 20-mV range around the reversal potential (E_{rev}), or from the chord conductance at various voltages. The data were analyzed using Clampfit (Axon Instruments, Inc.), Excel (Microsoft) and Sigmaplot (SPSS). Statistics were calculated using SigmaStat (SPSS)

After the oocyte recovered from impalement, CFTR was activated by adding a cocktail containing 10 μM forskolin and 1 mM 3-isobutyl-methylxanthine (IBMX; RBI) to the perfusate. Alternatively, when CFTR was coexpressed with the β-adrenergic receptor, isoproterenol (1–10 μM) and IBMX (1 mM) were used for activation. The β-adrenergic receptor has a number of endogenous cysteine residues that might be attacked by thiol reagents (Kobilka et al., 1987; Fraser, 1989; Javitch et al., 1997). We confirmed that the effects of thiol modification were similar in experiments with and without coexpression of the receptor. In addition, Javitch et al. (1997) showed that 2-(aminoethyl) methanethiosulfonate (MTSEA) had no effect on the binding of agonist or antagonist to wild-type β_2-adrenergic receptor expressed in HEK 293 cells. Rectification ratios were determined from the quotient of the slope conductance measured at +25 mV with respect to the reversal potential divided by the slope conductance measured at −25 mV with respect to the reversal potential.

Single-channel Recording

Single CFTR channels were studied in excised, inside-out patches at room temperature. Because preliminary experiments suggested that the single-channel conductance of unmodified R334C was much reduced from that seen with wt CFTR, we used

symmetric bathing solutions containing >200 mM Cl for these studies. Oocytes were prepared for study by shrinking in hypertonic solution (in mM: 200 monopotassium aspartate, 20 KCl, 1 $MgCl_2$, 10 EGTA, and 10 HEPES-KOH, pH 7.2) followed by manual removal of the vitelline membrane. Pipettes were pulled in four stages from borosilicate glass (Sutter Instrument Co.), and had resistances averaging ~10 MΩ when filled with pipette solution (in mM: 200 NMDG-Cl, 5 $MgCl_2$, and 10 TES, adjusted to pH 7.4 with Tris). Typical seal resistances were in the range of 200 GΩ. Channels were either activated on-cell with isoproterenol before excising into intracellular solution (200 NMDG-Cl, 1.1 $MgCl_2$, 2 Tris-EGTA, 1 MgATP, 10 TES, pH 7.3, and 50 U/ml PKA; Promega), or were activated by PKA after excision. Patch currents were measured with an amplifier (model AI2120; Axon Instruments, Inc.), and were recorded at 10 kHz on DAT tape (model DTC-790; Sony). For subsequent analysis, records were filtered at 100 Hz (4-pole Bessel filter; Warner Instruments) and acquired by the computer at 400 Hz using the Fetchex program of pClamp (Axon Instruments, Inc.). Fetchan and pSTAT were used to calculate open probability (P_o) at a membrane potential of −100 mV, where transitions were more easily distinguished, using records lasting between 36 and 113 s. Open and closed current levels were first identified manually, and then transition analysis using a 50% cut-off between open and closed levels was used. Only records from patches with low noise, and in which channel number could be clearly discerned, were used for this analysis. In most cases, channel activity before and after [2-(trimethylammonium)ethyl] methanethiosulfonate (MTSET) treatment was recorded from different oocytes. All but one record had two active channels in the patch; P_o values are presented for the first open level. The presence of multiple channels introduces error into the calculation of P_o, but this should have equal impact upon patches assayed before and after MTSET. Because the single-channel conductance of R334C CFTR before modification by MTSET was very small, we could not rely upon amplitude histograms for reliable estimation of channel amplitudes at varying membrane potentials. Instead, current amplitudes at several membrane potentials were measured manually using the Clampfit program for both pre- and postmodification records. Single-channel conductance was determined by linear regression. In a second set of experiments, MTSET was added to the patch pipette before seal formation and allowed to diffuse to the tip after seal formation, so that modification of R334C CFTR channels by MTSET could be monitored in real time. For this set of experiments, only patches containing a single-channel with low P_o were included in the analysis. To improve our ability to resolve single-channel currents, we used a Cl gradient such that the bath solution contained 300 mM NMDG-Cl and the pipette contained 30 mM NMDG-Cl and 270 NMDG-aspartate. The pipette was backfilled with the low Cl solution containing 100 μM MTSET. P_o was calculated as before.

Modeling and Curve Fitting

Two types of models were used to interpret the impact of charge changes at position 334 on anion conduction. In both the pore was viewed as comprising a rate-limiting central region flanked by "vestibule(s)" (Dani, 1986; Green and Andersen, 1991), where the electrical potential created by charged groups can influence local anion distribution. In one model, the properties of the rate-limiting region were described using a constant field, electrodiffusion model (Goldman, 1943) modified to incorporate charged inner and outer vestibules. The model was fitted to the data using the curve-fitting routines contained in SigmaPlot (SPSS). In the second model, the rate-limiting region was described using a 4-barrier, 3-well rate-theory scheme incorporating a variable surface potential in the outer vestibule. I-V plots were simulated using a program developed by Dr. Ted Begenisich (Begenisich and Cahalan, 1980,) and curves were fitted to the data by eye.

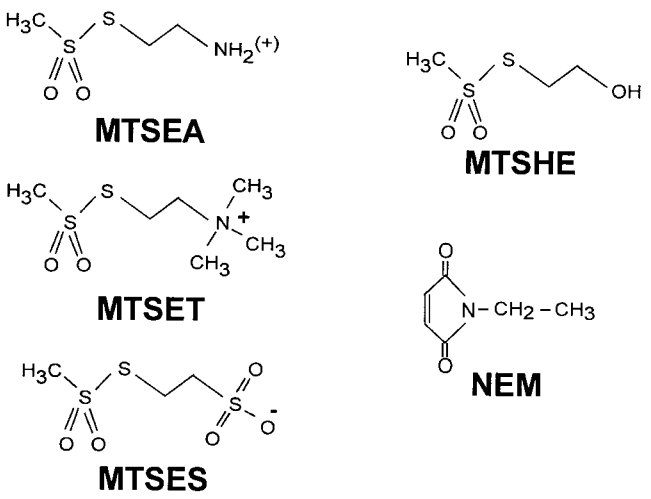

FIGURE 1. Chemical structures for the thiol-specific reagents used in this study.

The apparent pKa's for the titration-dependent changes in conductance with the histidine and cysteine substituted R334 variants were determined by assuming that the increase in charge was determined by the abundance of the protonated form of the histidine or cysteine and fitting the Henderson-Hasselbach equation to the data as follows:

$$\%g = \frac{\%g_{max}}{1 + e^{2.303(pH - pKa)}}, \quad (1)$$

where %g is the percent increase in conductance with respect to that measured in the most basic solution used in a particular experiment (typically pH 9–10). pH is the bath pH determined from repeated measures with at least two different electrodes, $\%g_{max}$ is the maximum change in conductance that would be observed if the site were fully protonated (determined from the regression), and pKa is the apparent pKa determined from the regression.

Reagents

The following thiol-specific modifying reagents were used in these studies: MTSEA, MTSET, 2-sulfonatoethyl methanethiosulfonate (MTSES), 2-hydroxyethyl methanethiosulfonate (MTSHE), and *N*-ethylmaleimide (NEM). Structures for these reagents are shown in Fig. 1. All MTS reagents were purchased from Toronto Research Chemicals Inc. For concentrations >1 mM, they were directly suspended immediately before use; however, for concentrations <1 mM, the reagent was first suspended in deionized water, aliquoted and frozen at −20°C and thawed and diluted immediately before use. The reducing agent dithiothreitol was purchased from Molecular Probes. 2-Mercaptoethanol (2-ME) and all other reagents were purchased from Sigma-Aldrich.

RESULTS

Bath-applied MTS Reagents Did Not Alter the Functional Properties of wt CFTR

The CFTR constructs used in these studies contain 18 endogenous cysteines, four of which are located in the

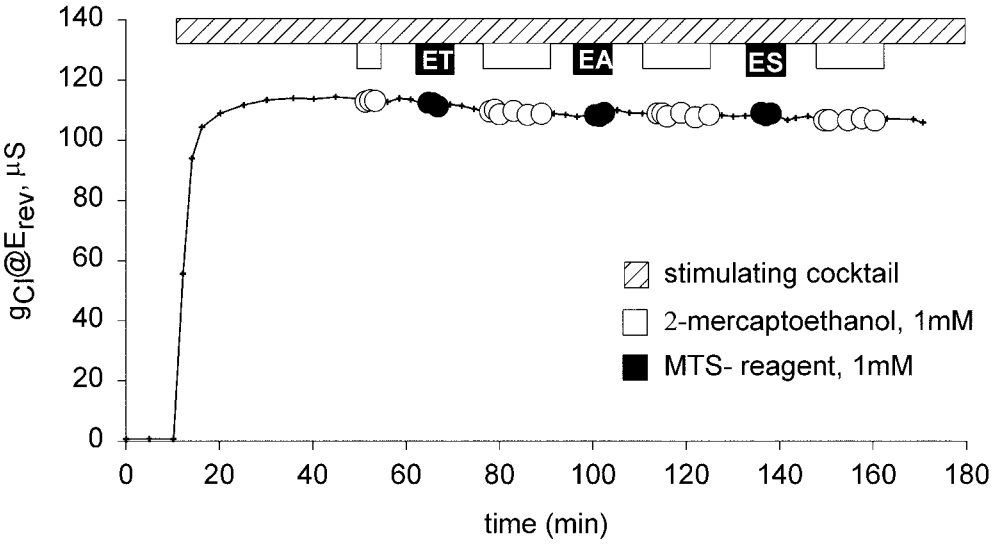

FIGURE 2. MTS reagents did not alter the function of wt CFTR expressed in oocytes. Conductance ($@E_{rev}$) is plotted versus time. After CFTR was activated by the application of 1 mM IBMX and 10 μM forskolin (hatched bar; see MATERIALS AND METHODS), oocytes were exposed sequentially to 1 mM 2-ME (white bars and circles), 1 mM MTSET, MTSEA, and MTSES (black bars and circles).

putative transmembrane segments (C128, C225, C343, and C866). Hence, it was important to determine if any of the modifying reagents produced alterations in the channel function of wt CFTR. Fig. 2 contains the results of a representative experiment for which total membrane conductance ($@E_{rev}$) of an oocyte expressing wt CFTR is plotted versus time. After the conductance achieved steady-state activation during exposure to a stimulating cocktail containing 10 μM forskolin and 1 mM IBMX, the oocyte was exposed to 1 mM 2-ME, followed by a 10-min wash, then a 3-min exposure to 1 mM MTSET, followed by a 10-min wash and exposure to 2-ME for 12 min, followed by another 10-min wash. A similar protocol was used to expose the oocyte to MTSEA and MTSES. The experiments were repeated with each of the compounds individually, both with and without prior exposure to 2-ME. It can be seen that neither the 2-ME nor any of the MTS reagents produced any significant change in the conductive properties of wt CFTR. On occasion, a slight increase (<5%) in conductance was elicited with applications of MTSEA in concentrations of 1 mM or greater, but not with concentrations of 100 μM or less. Although not shown here, we also tested oocytes expressing wt CFTR for an impact of reagents on the response to step changes in clamping potential and for changes in I-V shape and found no discernible effects of MTSES and MTSET (even when they were used in millimolar concentrations) on Cl conductance. It must be emphasized that this does not mean that the endogenous cysteines were not being modified, only that modification, if it occurred, did not result in an alteration of function that was discernible in this experimental setting. A similar lack of functional effects of MTS reagents on wt CFTR was reported by Cheung and Akabas (1996).

The Function of R334C and K335C CFTR Was Modified by External MTSES or MTSET but the Function of R347C and R352C CFTR Was Not Modified by these Polar Thiol Reagents

Fig. 3 summarizes the results of experiments in which MTSES, MTSET, or MTSEA (100 μM–10 mM) were added to the solution bathing oocytes expressing wt, R334C, K335C, R347C, or R352C CFTR. Plotted is the percent change in conductance ($@E_{rev}$) before and after a 1–3-min exposure to MTS reagents applied after steady-state activation was achieved. The data were derived from experiments such as those shown in Figs. 2–6 and 8.

For both R334C and K335C CFTR, the results of modification by the negatively charged reagent (MTSES) generally agreed with those reported by Cheung and Akabas (1996). For R334C CFTR, they reported ~40% decrease in the normalized current (@ –100 mV) and we observed ~70% decrease in the conductance ($@E_{rev}$). For K335C, they reported ~13% decrease in the normalized current (@ −100 mV) and we observed ~30% decrease in the conductance ($@E_{rev}$).

In the case of the positively charged reagents (MTSET and MTSEA), we obtained distinctly different results. Cheung and Akabas (1996) reported that application of 1 mM MTSET to oocytes expressing R334C CFTR reduced the normalized current (@ −100mV) by ~54%, and 2.5 mM MTSEA reduced the normalized current by ~35%. In contrast, we found that the application of 100 μM or 1 mM MTSET to oocytes expressing R334C CFTR resulted in ~110% increase in the conductance, whereas 100 μM or 1 mM MTSEA increased the conductance by ~70%. For K335C CFTR, Cheung and Akabas (1996) reported that the application of 2.5 mM MTSEA resulted in ~20% decrease in the normalized current (@ −100 mV), whereas we observed ~20% increase in the conductance ($@E_{rev}$). Thus, the two stud-

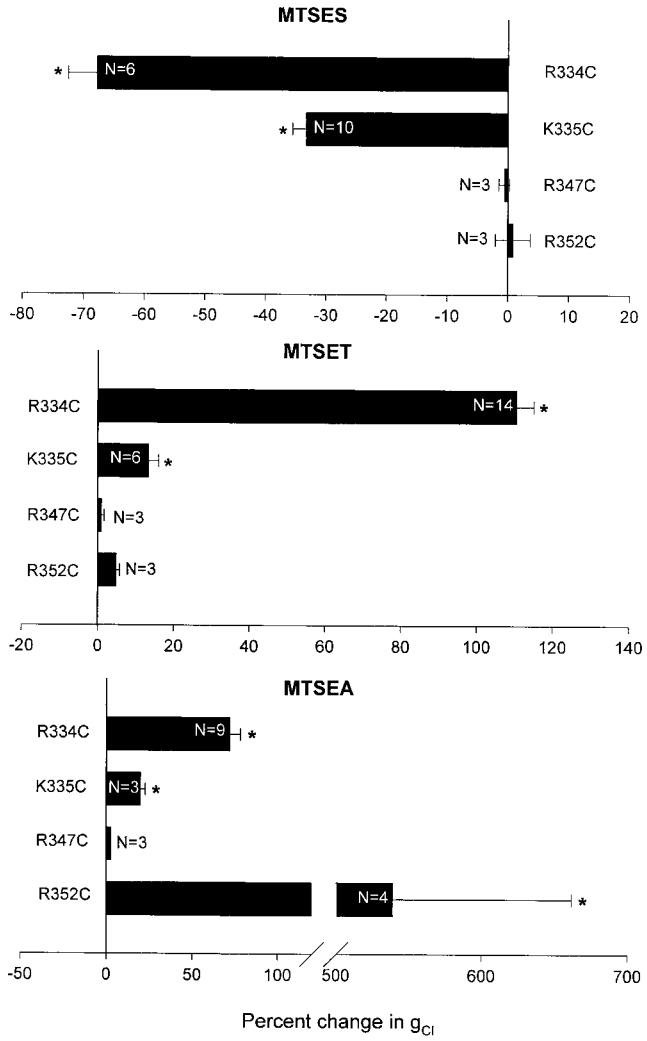

FIGURE 3. Comparison of the effects of MTSES, MTSET, and MTSEA on the conductance of oocytes expressing R334C, K335C, R347C, or R352C CFTR. Plotted are values for the percent change in oocyte conductance ($\Delta g/g_{initial} \times 100\%$) induced by each reagent (±SEM). Asterisk indicates significant difference from unmodified conductance, $P < 0.05$.

ies are in accord as regards accessibility, but differ qualitatively as to the nature of the functional effect.

Shown in Fig. 4 is a representative experiment in which an oocyte expressing R347C CFTR was exposed to MTS reagents. After the oocyte achieved steady-state activation during exposure to stimulating cocktail, it was exposed to 1 mM 2-ME, followed by a 10-min wash, then a 3-min exposure to 1 mM MTSET, followed by a 10-min wash and exposure to 2-ME for 12 min, followed by another 10-min wash. A similar protocol was used to expose the oocyte to MTSEA and MTSES. The experiments were repeated with each of the compounds individually, both with and without prior exposure to 2-ME and in no case were we able to detect an effect on the function of R347C CFTR. Cheung and Akabas (1996) initially reported that there was a ~50% decrease in the normalized current (@ −100 mV) after exposure of oocytes expressing R347C CFTR to 10 mM MTSES, 1 mM MTSET or 2.5 mM MTSEA. However, in the course of subsequent studies by Cheung and Akabas (1997), it was discovered that the R347C construct had a substantial deletion. MTSES or MTSET were reported as not reacting with the full-length R347C CFTR, and MTSEA was reported to cause a 19% inhibition. Tabcharani et al. (1993) had identified R347 as a potential pore-lining residue based on the effects of mutations on SCN binding, but Cotten and Welsh (1999) proposed that R347 forms a salt bridge with D924.

In the case of R352C CFTR, our observations also differed substantially from those reported by Cheung and Akabas (1996, 1997). They reported that exposing oocytes expressing R352 CFTR to 10 mM MTSES resulted in ~30% decrease in the normalized current (@ −100 mV), whereas 2.5 mM MTSEA caused ~25% decrease and 1 mM MTSET resulted in ~50% decrease. In contrast, we were not able to detect effects of this magnitude applying either MTSES or MTSET to oocytes expressing R352C CFTR (Fig. 5 A). Although not apparent in the

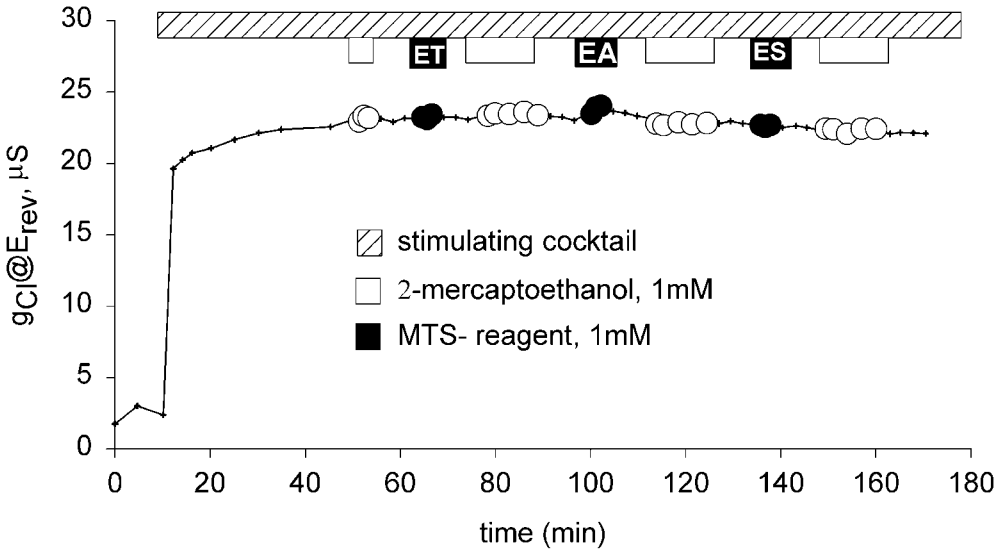

FIGURE 4. MTS reagents did not discernibly alter the function of R347C CFTR expressed in oocytes. Protocol as in Fig. 2.

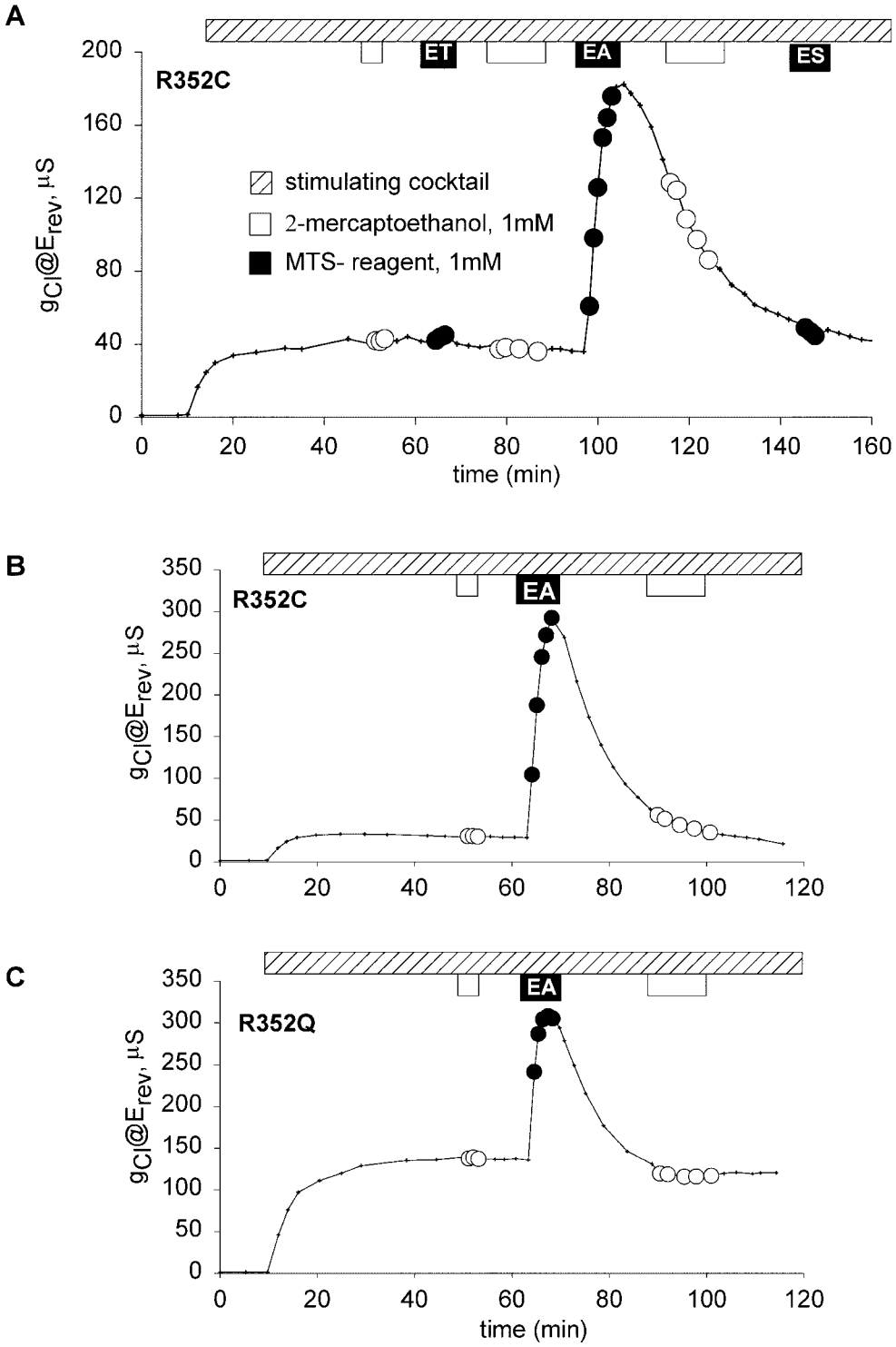

FIGURE 5. MTSET and MTSES, polar thiol reagents, did not produce a discernible alteration in conductance of oocytes expressing R352C CFTR. Protocol as in Fig. 2. (A) Application of 1 mM 2-ME, 1 mM MTSET, or 1 mM MTSES produced no discernible change in conductance. 1 mM MTSEA produced a nearly fivefold increase in conductance, which spontaneously reversed when MTSEA was removed from the perfusate. (B) Addition of 1 mM MTSEA produced a sixfold increase in conductance of an oocyte expressing R352C CFTR not previously exposed to MTSET. The effect spontaneously reversed when MTSEA was removed from the perfusate. (C) MTSEA produced a twofold increase in conductance in an oocyte expressing R352Q CFTR, which spontaneously reversed when MTSEA was removed from the perfusate.

record shown, we have noted small (2–5%) changes in the conductance when these oocytes were exposed to 1 mM MTSET. Changes of this magnitude are also seen in oocytes expressing R352Q or R352H CFTR, but were not seen in oocytes expressing wt CFTR. This result could reflect a labeling event that is without major functional effect in this assay. However, it is unlikely that any effect can be attributed to the cysteine that is substituted for R352 (see next section; Fig. 5, A and B).

R352C CFTR Function Is Modified by Addition of 1 mM MTSEA to the Perfusate, However the Effect Is Not Cysteine-specific

Shown in Fig. 5 B is the result of a representative exper-

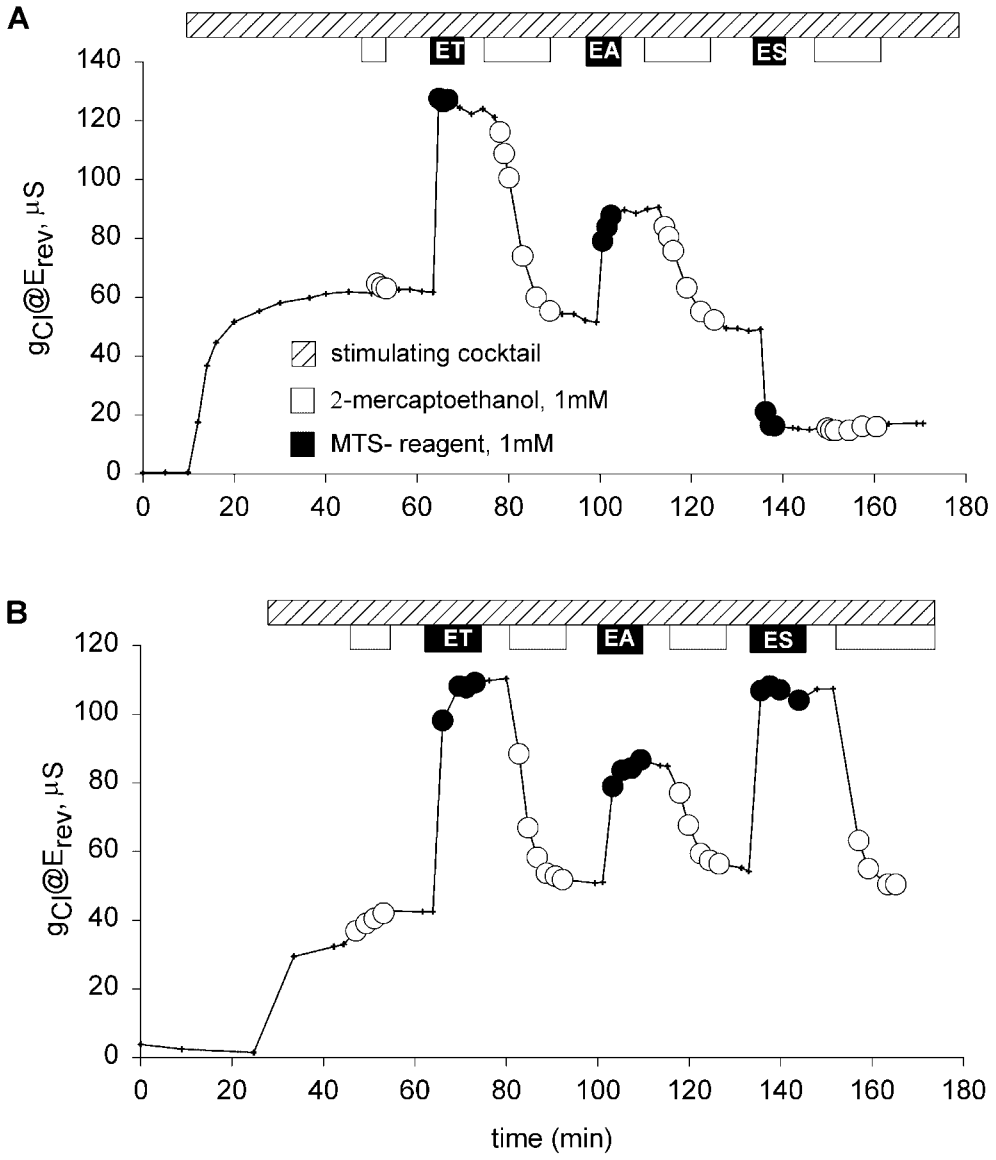

FIGURE 6. Covalent modification of R334C CFTR was stable, reproducible, and varied with the electrostatic nature of the moiety covalently attached. Protocol as in Fig. 2. (A) Exposure to 1 mM MTSET resulted in doubling of the conductance, which remained elevated until the oocyte was exposed to 2-ME. 1 mM MTSEA resulted in an increase in conductance which was ~70% of the increase elicited by MTSET, and was stable until the application of 2-ME. MTSES reduced the conductance to ~30% of the unmodified level. Modification was stable and not readily reversed by the application of 1 mM 2-ME at pH 7.4. (B) Reapplication of MTSET reproduced the effects seen with the first application.

iment in which an oocyte expressing R352C CFTR was exposed to 1 mM MTSEA; the result being a sixfold increase in conductance. The fact that a response was obtained only with a reagent known to permeate cell membranes (Holmgren et al., 1996) suggested that MTSEA accessed its site of action by entering the oocyte (or plasma membrane). Consistent with such a view, we found that after removing the reagent from the perfusate, the reaction spontaneously reversed over a period of 30 min, as expected if endogenous reducing agents, such as glutathione and free cysteine, were breaking the disulfide bond. In contrast, exposure of an oocyte expressing R334C CFTR to 1 mM MTSEA for 3 min produced an increase in conductance that remained elevated after washing out the reagent until a reducing agent, 1 mM 2-ME, was added to the perfusate (see Fig. 6 A).

Importantly, we also obtained a transient response to the application of MTSEA in oocytes expressing R352Q CFTR (Fig. 5 C) or R352H CFTR (unpublished data). This result strongly suggests that MTSEA was reacting with an endogenous cysteine that was rendered either accessible or functionally significant as a result of amino acid substitution for R352. We have not yet identified the endogenous cysteine, however, and cannot exclude the possibility that the cysteine in question was accessible to MTSEA in the absence of substitution at position 352 (i.e., wt CFTR), but that modification was without functional impact. Guinamard and Akabas (1999) reported that substitutions for R352 (C, Q, and H) decreased the Cl^-/Na^+ selectivity of CFTR as determined in detached patches (CHO cells), but we did not detect any alteration in the reversal potential associated with the expression of R352Q or H CFTR in oocytes.

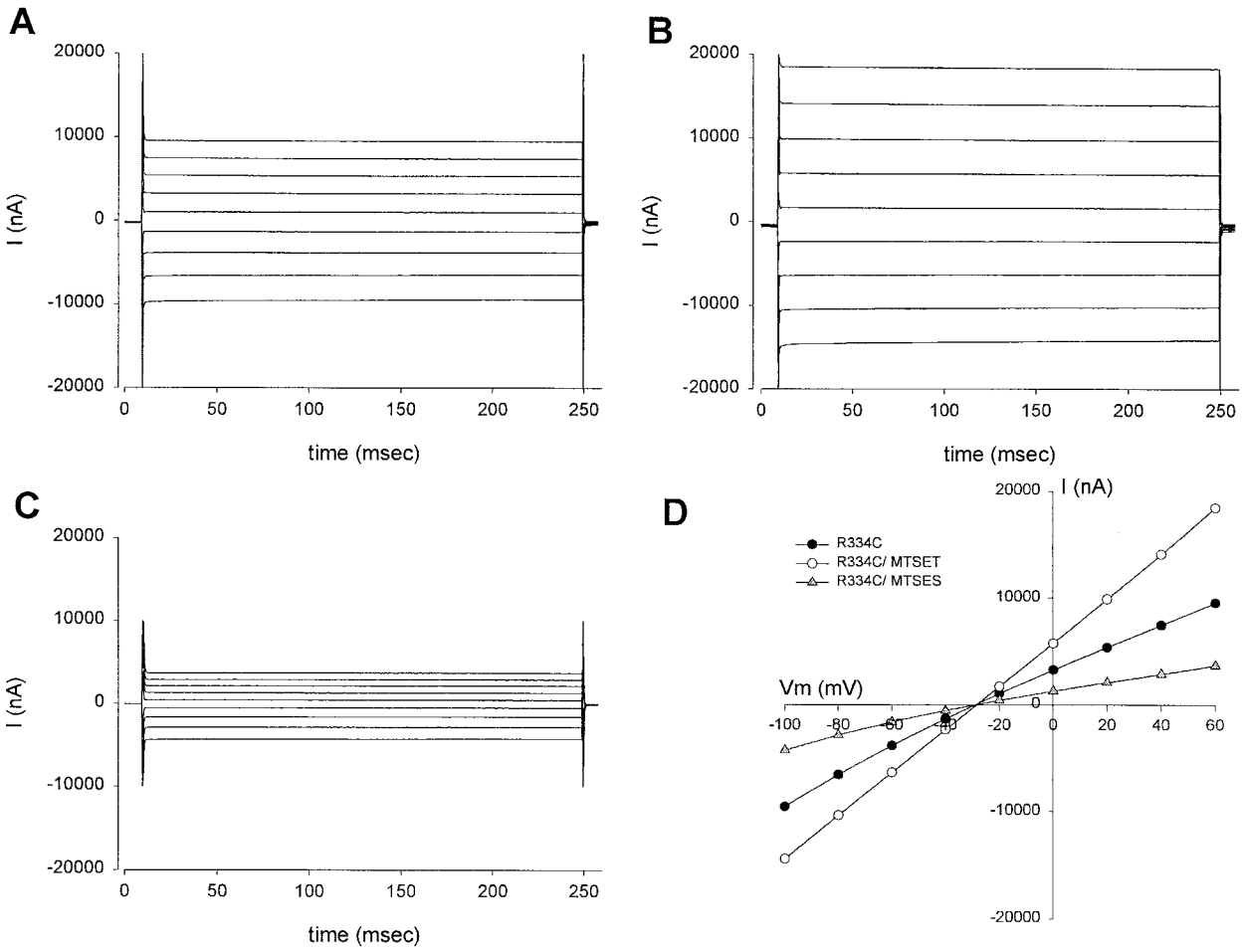

FIGURE 7. R334C CFTR did not exhibit time-dependent current relaxations. (A) Currents evoked by stepping the potential from −100 to +60 mV for 234 ms from an oocyte expressing R334C CFTR after achieving steady-state activation with stimulatory cocktail and after a brief (3 min) exposure to 1 mM 2-ME. (B) Currents from the same oocyte after modification with 100 μM MTSET. (C) Currents from the same oocyte after a 12-min exposure to 1 mM 2-ME to reverse the MTSET modification followed by exposure to 100 μM MTSES. (D) I-V plots derived from the current traces shown in A–C: (closed circles) unmodified R334C CFTR; (open circles) MTSET modified R334C CFTR; and (closed triangles) MTSES modified R334C. There were readily detectable changes in the conductance and the shape of the I-V relation, but no shift in the reversal potential.

The Effects of Polar MTS Reagents Applied to R334C and K335C CFTR Were Stable and Readily Reversible with 2-ME, which Is Consistent with the Formation of a Mixed Disulfide Bond

The results of an experiment in which an oocyte expressing R334C CFTR was exposed to multiple MTS reagents and 2-ME are shown in Fig. 6 A. The addition of 1 mM MTSET to the bath resulted in a doubling of the conductance ($@E_{rev}$). The conductance remained elevated in the presence of reagent-free solution, and the addition of 2-ME to the bath resulted in a decrease in the conductance to the level seen before MTSET modification. The application of 1 mM MTSEA resulted in an increase in conductance; however, the magnitude was less than the increase seen with MTSET. This result could be a reflection of the difference in the charge-bearing moiety associated with MTSET and MTSEA. The TEA group of MTSET, like other quaternary ammonium compounds, is expected to be fully ionized and quite stable (Solomons and Fryhle, 2000). The result seen with MTSEA in this experimental setting could reflect less than complete ionization of the primary amine as well as a difference in the geometry of the added charge. Holmgren et al. (1996) reported that whereas MTSET did not permeate lipid membranes, MTSEA was membrane permeant, as if a significant portion of the compound existed in the nonionic form. The pKa of MTSEA is not known, although it has been estimated to be around 8.5 (Karlin and Akabas, 1998). The difference between MTSET and MTSEA in the experiment shown was not due to the multiple exposure protocol; a second exposure to MTSET reproduced the effects seen with the first (Fig. 6 B).

The deposition of a negative charge at R334 (MTSES) resulted in a decrease in the conductance (Fig. 6 A). The modification with MTSES was poorly reversible with the reducing agent 2-ME at pH 7.4. However, it was possible to reverse the modification of R334 CFTR with negatively charged reagents under alkaline conditions (pH 9.0; unpublished data), which increases the abundance of the thiolate anion (Singh et al., 1995).

In view of the results obtained with R352C CFTR, we tested for effects of exposure to MTSET and MTSES using constructs bearing substitutions other than cysteine for R334. MTSES, MTSET, or MTSEA (100 μM or 1 mM) were added to the perfusate of oocytes expressing R334A or R334Q CFTR and produced no discernible effect on conductance (unpublished data). Only R334C exhibited an altered conductance in response to thiol-reactive reagents, which is consistent with the working hypothesis that the observed changes were due to the chemical modification of the cysteine substituted for R334.

The Modification of R334C and K335C CFTR by MTS Reagents Altered Both the Conductance and the Shape of the Current-Voltage Plot

In the course of these experiments, it became apparent that a change in conductance of oocytes expressing either R334C or K335C CFTR induced by exposure to MTSET or MTSES was always accompanied by a concomitant change in the shape of the I-V plot. Therefore, we conducted a series of experiments in which changes in conductance were compared with changes in I-V shape, quantified as the rectification ratio (RR), where RR was defined as the ratio of the slope conductance calculated 25 mV positive to E_{rev} to that calculated 25 mV negative to E_{rev} (Mansoura et al., 1998). Shown in Fig. 7 are the results of a representative experiment in which currents were elicited by step changes in clamping potential from −100 mV to +60 mV for either the unmodified (A), MTSET modified (B), or MTSES modified R334C CFTR (C), and the resulting I-V plots (D). The addition of 100 μM MTSET to the perfusate resulted in an increase in the current measured at all potentials. The conductance ($@E_{rev}$) increased by 74%, and the shape of the I-V plot went from mild inward rectification (RR = 0.85) in the unmodified state to linear (RR = 1.01) after modification with 100 μM MTSET. There was no change in the reversal potential (−27 mV). The currents elicited after reversal of the MTSET modification by 1 mM 2-ME were indistinguishable from the currents before MTSET modification. The addition of 100 μM MTSES to the perfusate resulted in a decrease in the amplitude of the current measured at all potentials. The conductance ($@E_{rev}$) decreased by 59% and the inward rectification became more pronounced (RR = 0.77), but there was no change in the reversal potential. The currents in the unmodified and modified states, like the currents elicited from wt CFTR, did not exhibit any time-dependent relaxation, as might be expected if charge addition altered or induced voltage-dependent gating. In addition, measurements using voltage steps (shown here) and voltage ramps (positive and negative; unpublished data) resulted in identical values for RR.

Fig. 8 A contains the results of a representative experiment in which the total membrane conductance ($@E_{rev}$) of an oocyte expressing K335C CFTR was measured as a function of time. After achieving steady-state activation, 2-ME (1 mM) was added to the bath and produced a slight increase in conductance. This conductance level was stable during a subsequent 10-min wash with stimulating cocktail alone. Addition of 1 mM MTSET to the bath resulted in an ∼15% increase in conductance. The conductance remained elevated during a subsequent 10-min wash with stimulating cocktail alone and a 12-min exposure to 2-ME resulted in a decrease in the conductance to the level seen before MTSET modification. Addition of 1 mM MTSEA to the bath resulted in an increase in conductance (∼20%), which remained elevated until 2-ME was added to the bath. In contrast, the addition of 1 mM MTSES, a negatively charged reagent, resulted in ∼30% decrease in the conductance and a discernible alteration in the shape of I-V plot from slight outward rectification to modest inward rectification (Fig. 8 C). In Fig. 8 B, the rectification ratio is plotted versus time for the same oocyte demonstrating that the change in conductance and the change in the shape of I-V plot were highly correlated. As indicated above, modification by MTSES was very poorly reversible with 1 mM 2-ME at pH 7.5, and as with R334C, current relaxations in response to voltage steps were not detected in either the modified or unmodified state. The results of covalent modification were qualitatively similar for K335C and R334C CFTR, but the greater magnitude of the effects for the latter construct led us to focus further studies on modification and substitution at position 334.

Because changes in the shape parameter, RR, emerged as an important component of the response to charge changes, we investigated the possibility that the changes in I-V shape were an artifact of inadequate voltage control or some other effect of increased oocyte conductance (Baumgartner et al., 1999). As a control for possible series resistance errors that might distort I-V shape or apparent conductance, we compared the change in conductance and RR caused by MTSET in oocytes for which the conductance varied over wide range due either to oocyte-to-oocyte variation in expression or to differential activation of CFTR. Fig. 9 A shows the activated conductance of oocytes expressing R334C CFTR measured just after modification by MTSET plotted against that measured just before modifi-

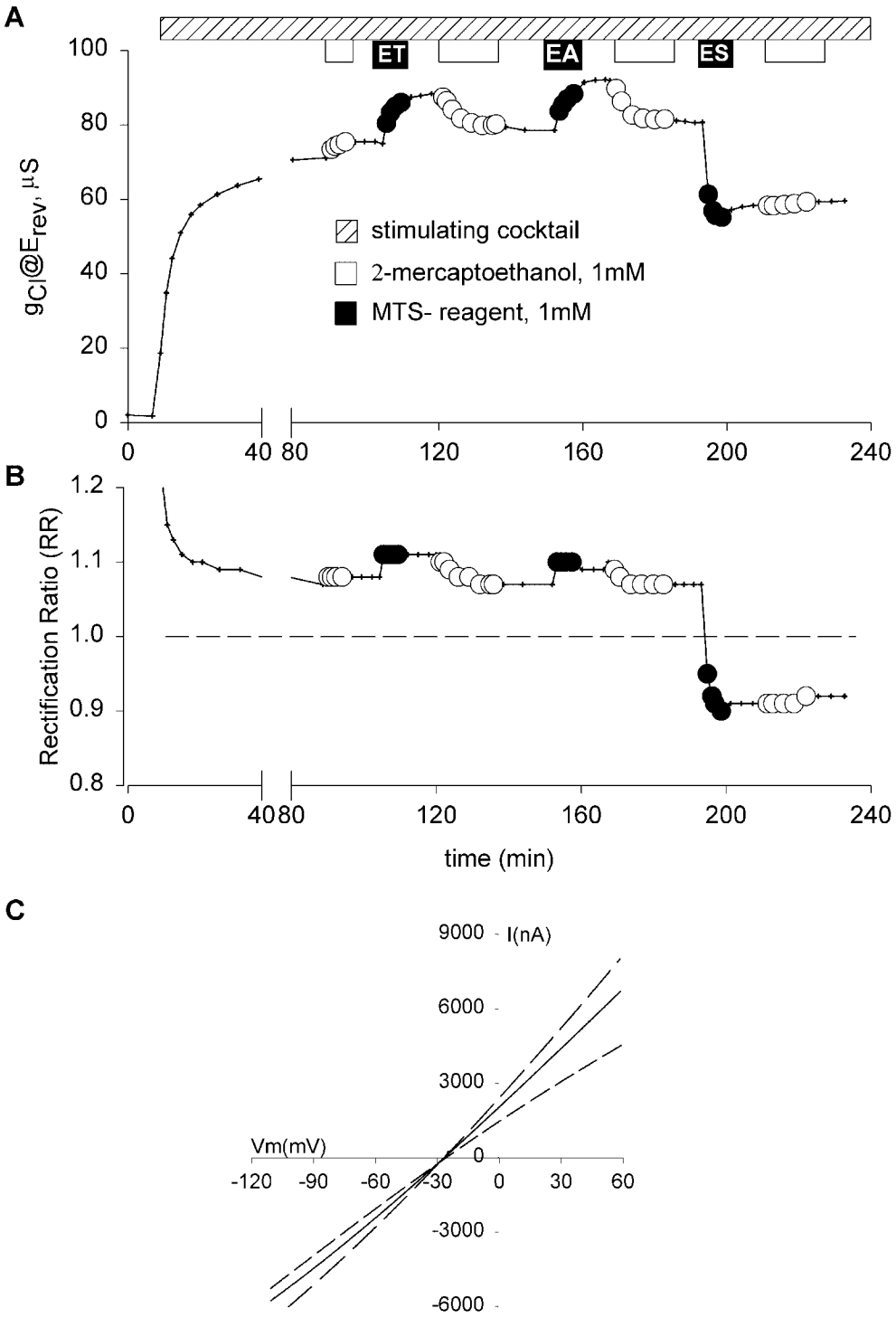

FIGURE 8. Covalent modification of K335C CFTR altered both conductance and shape of the I-V relation. Protocol as in Fig. 2. (A) The oocyte was exposed to 2-ME (white bars) and MTS reagents (black bars). Positively charged reagents (MTSET and MTSEA) increased conductance and were readily reversed by 2-ME. The negatively charged reagent (MTSES) resulted in a ~30% decrease in the conductance and was poorly reversible with 1 mM 2-ME at pH 7.4. (B) The rectification ratio (RR)—quantified as the slope conductance measured at +25 mV with respect to E_{rev} divided by the slope conductance measured at E_{rev} – 25 mV—plotted versus time for the same oocyte. RR of unity reflected a linear I-V relation and is noted with a dashed line. RR values greater or less than unity indicate outward and inward rectification, respectively. (C) I-V plots for K335C CFTR before and after application of MTS reagents. (solid line) Before modification; (dotted line) after treatment with MTSET; (dashed line) after treatment with MTSES. There were changes in the conductance and the shape of the current-voltage relation, but no shift in reversal potential.

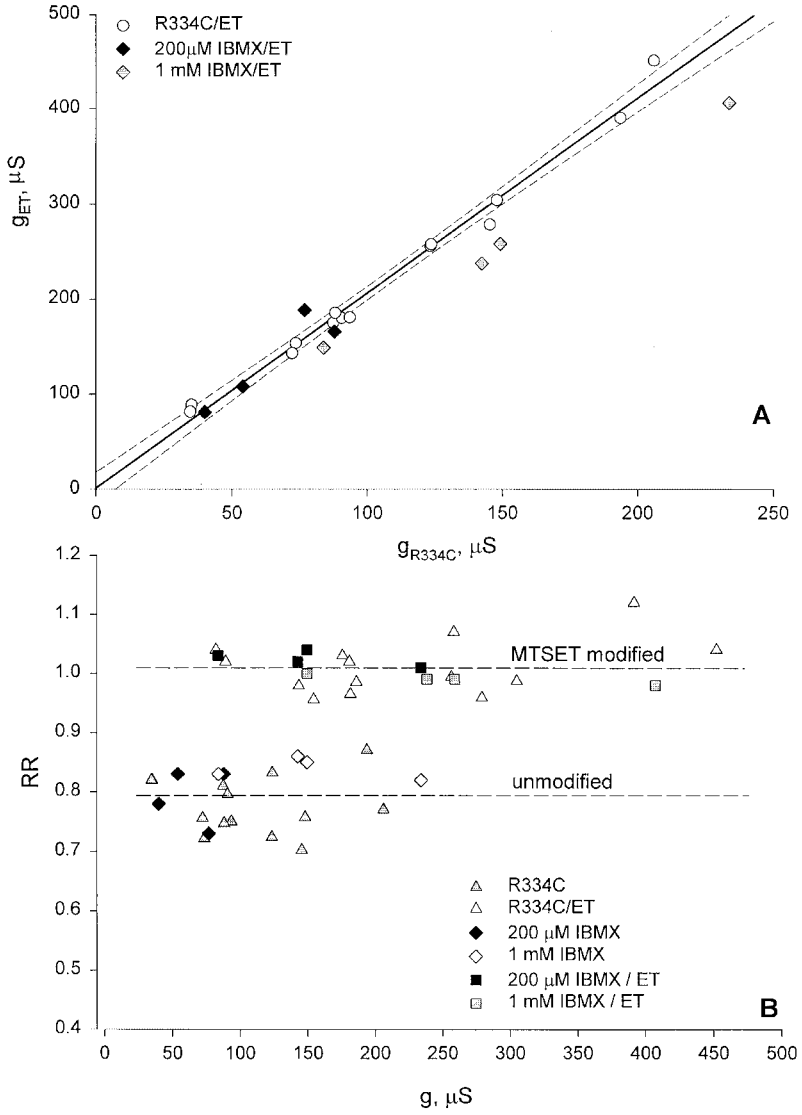

FIGURE 9. Changes in conductance and I-V shape induced by MTSET were not dependent on oocyte conductance or the activation state of CFTR. (A) Conductance of oocytes expressing R334C CFTR determined just after modification by MTSET plotted versus premodification conductance. Dashed line is least-squares fit to open circles, representing oocytes activated using 1 mM IBMX and 10 μM isoproterenol (slope equals 2.05, r = 0.987), dashed lines (95% confidence limits). (dark diamonds) Oocytes activated using 200 μM IBMX; (gray diamonds) oocytes after reversing MTSET modification, activation by 1 mM IBMX, and reexposure to MTSET. (B) Values of RR plotted versus corresponding oocyte conductance. (open and closed triangles) Oocytes activated using 1 mM IBMX, 10 μM isoproterenol. (closed and open diamonds) Oocytes exposed sequentially to 200 μM and 1 mM IBMX, in the absence of MTSET. (closed and open squares) Oocytes activated by 200 μM IBMX, 10 μM isoproterenol, exposed to MTSET and, after reversing MTSET (2-ME), activated again using 1 mM IBMX and reexposed to MTSET. Dashed lines are mean values of RR for modified and unmodified R334C CFTR.

cation. The dashed line is the least-squares fit to the open circles, which represent oocytes activated by 1 mM IBMX and 10 μM isoproterenol. The slope of the line is 2.05 and the intercept is near 0, indicating that over the range of 50–250 μS the effect of covalent modification was similar and, at pH 7.4, approximately doubled the conductance due to R334C CFTR. Also shown are several determinations made after activation by 200 μM IBMX that yields approximately half-maximal activation of R334C CFTR (Wilkinson et al., 1996; Mansoura et al., 1998). The effect of MTSET was identical at the reduced level of activation. The third set of points represents the latter set of oocytes after reversing MTSET modification (2-ME), activating with 1 mM IBMX and exposing to MTSET for a second time. It is apparent that the increase in conductance resulting from the second exposure to MTSET was somewhat less than the first. The source of this difference is unclear at present, but may represent the failure of the reducing agent to completely reverse the initial covalent modification of CFTR.

Fig. 9 B contains values of RR measured before and after modification plotted versus the conductance corresponding to each state. RR determined either before or after covalent modification did not vary in any systematic way with the conductance of the oocyte, suggesting that the changes in this parameter induced by covalent modification were not an artifact of inadequate voltage control. It can be seen that changes in RR due to MTSET modification at a reduced level of activation (200 μM IBMX) were similar to those seen at 1 mM IBMX. Increasing conductance by raising the concentration of IBMX from 200 μM to 1 mM did not alter RR.

Covalent Modification of R334C by MTSET Was Detectable as an Increased Single-channel Conductance

The results of experiments in which single-channel currents were recorded before and after R334C CFTR was

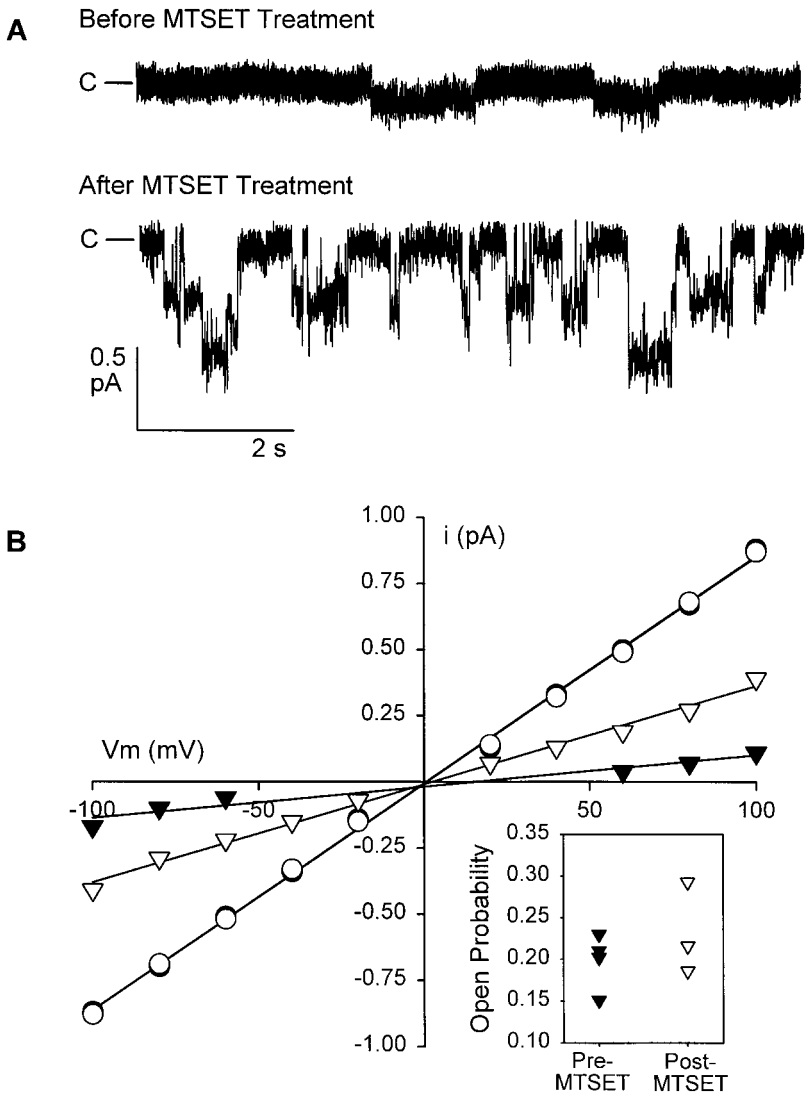

FIGURE 10. Covalent modification of R334C increased single-channel conductance. (A) Representative traces from an oocyte expressing R334C CFTR in the detached, inside-out patch configuration, $V_m = -80$ mV. The top trace was recorded before treatment with MTSET. The bottom trace was recorded from a separate patch on the same oocyte, after a 6-min exposure to 100 μM MTSET in the bath before establishing the seal. Channels were activated by the addition of 10 μM isoproterenol to the bath, before excising into the intracellular solution (see MATERIALS AND METHODS) containing 1 mM MgATP and 50 U/ml PKA catalytic subunit. Bath and pipette solutions contained ~210 mM Cl. The patch represented by the top trace contained only one active channel, whereas the lower patch contained two channels. Closed current level is indicated. (B) I-V plot for pooled single channel records ($n = 4$, pretreatment and $n = 3$, post-treatment). Standard errors are smaller than the symbols used. The solid lines are the best fit to the data by linear regression and correspond to a single-channel conductance of 1.2 pS for unmodified R334C CFTR (closed triangles) channels and 3.7 pS after MTSET modification (open triangles). MTSET did not alter single-channel conductance of wt CFTR (8.6 pS, open and closed circles). Inset shows open probability for R334C CFTR channels at $V_m = -100$ mV before and after treatment with MTSET (see MATERIALS AND METHODS). There was no significant change in P_o after treatment ($P = 0.361$, t test).

exposed to MTSET are shown in Fig. 10. The single-channel conductance of R334C CFTR was quite low (~1.2 pS, Fig. 10 A) even in the presence of elevated bath Cl concentration (210 mM). After exposure to MTSET, the single-channel conductance increased to 3.7 pS (Fig. 10 B). This result is consistent with the notion that the charge at position 334 is an important determinant of pore conductance. Also shown in the figure are points representing single-channel currents recorded from oocytes expressing wt CFTR that, under the same experimental conditions, exhibited a single-channel conductance of 8.6 pS and was unaffected by exposure to external MTSET.

The inward rectifying I-V shape characteristic of the macroscopic currents recorded from oocytes expressing unmodified R3334C CFTR was not apparent in single-channel currents recorded from detached patches (Fig. 10 B). The small size of the single-channel currents and the differences in experimental conditions under which single-channel and macroscopic currents were recorded makes it difficult to interpret this difference, but we cannot exclude the possibility that some intracellular constituent that is not present when patches of membrane are detached contributes to the rectification seen in intact oocytes.

The inset to the I-V plot (Fig. 10 B) shows the distribution of open probabilities calculated for individual R334C CFTR channels recorded from patches detached either before or after exposure to MTSET. The open probabilities for the two groups were overlapping, and statistical analysis indicated that they were not significantly different ($P = 0.361$). However, in these experiments, comparisons were made using patches detached either from the same or different oocytes before and after exposure to MTSET, so that there was a large variation in gating between patches that was unrelated to covalent modification. As a more rigorous test for possible effects of covalent modification on P_o, we monitored the modification of individual R334C CFTR channels using pipettes backfilled with a solution containing 100 μM

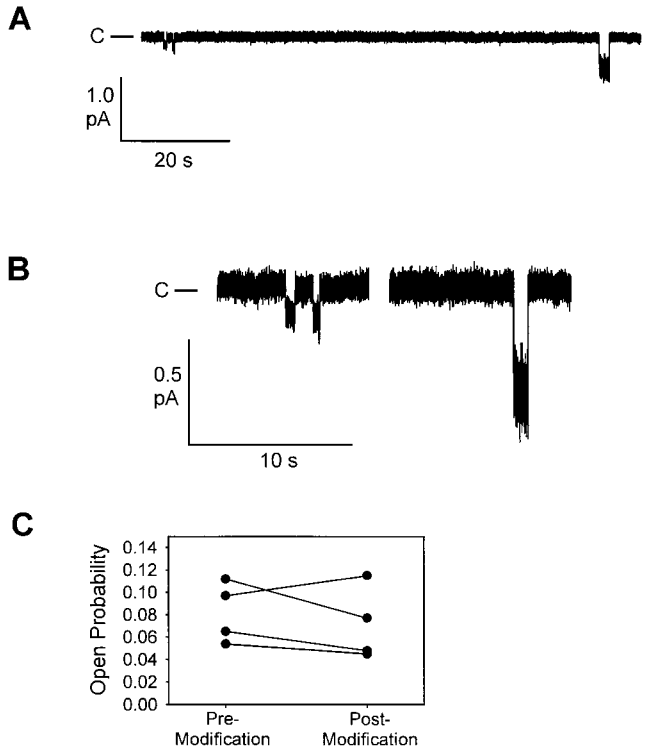

FIGURE 11. Covalent modification of a single R334C CFTR channel in real time by including MTSET in the patch pipette. (A) Openings in a detached patch before and after modification which occurred at some time during the 75-s separating the last low amplitude opening and the first higher amplitude opening. $V_m = -100$ mV, $[Cl]_{cyto} = 300$ mM and $[Cl]_{pipette} = 30$ mM. (B) Openings from the same record with scale expanded. (C) P_o determined before and after covalent modification for four, single R334C CFTR channels. Modification was assumed to have occurred at the midpoint between the last unmodified and first modified openings. Each value represents 3–5 min before and after modification.

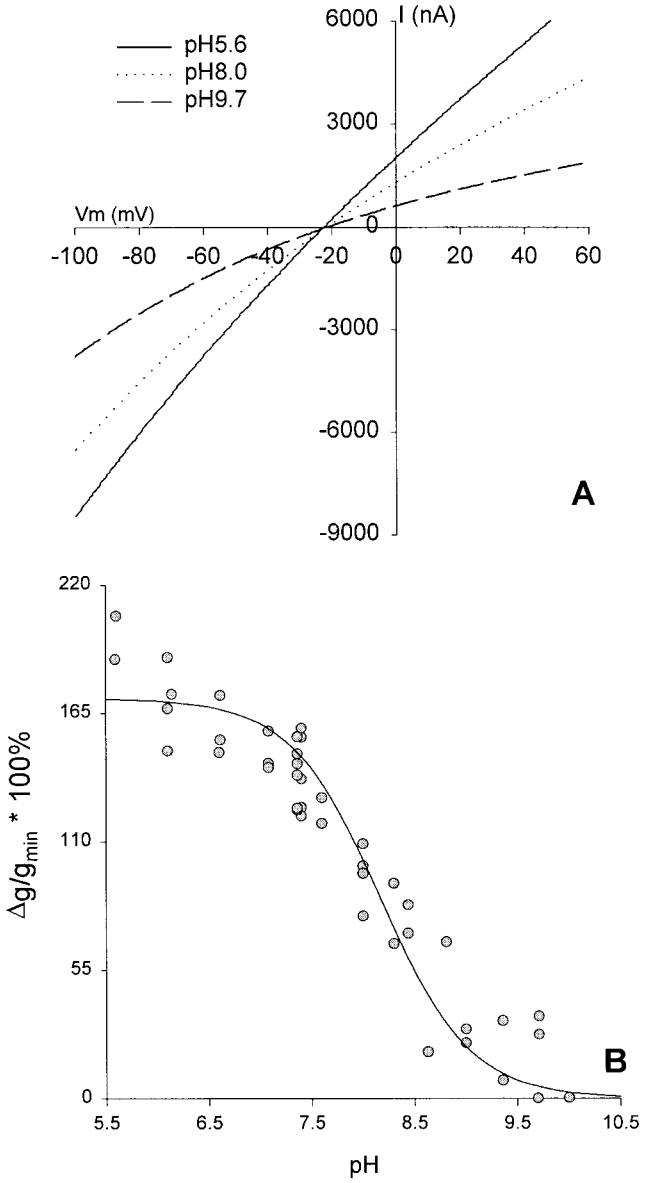

FIGURE 12. pH titration of oocytes expressing R334C CFTR altered both the conductance and the shape of the I-V relation. (A) I-V plot from an oocyte expressing R334C CFTR. After achieving steady-state activation in stimulatory cocktail at pH 7.4, the bath was acidified to pH 5.6 (solid line). Alkalinization of the bath to pH 8.0 (dotted line) or pH 9.7 (dashed line) decreased conductance and enhanced inward rectification without altering the reversal potential. (B) Percent increase in conductance with respect to the lowest conductance observed (most alkaline pH) plotted versus the bath pH for three different oocytes. Eq. 1 was fitted to points from 5.6 to 10.0, and resulted in a mean pKa of 8.17 ± 0.10 (SEM) and a mean $\%g_{max}$ of 170 ± 6.9 (SEM). The solid line represents the Henderson-Hasselbach equation for a pKa of 8.17.

MTSET. Fig. 11 (A and B) contains a result representative of that obtained in four experiments. Cl^- concentration in the bath was raised to 300 mM and that in the pipette reduced to 30 mM to enhance single-channel resolution. Immediately after detaching the patch into a solution containing PKA and ATP, single channels exhibited the low conductance characteristic of R334C CFTR. Over the course of ~10 min, the channel was modified by MTSET diffusing into the tip of the patch pipette, as indicated by the increase in the single-channel amplitude. Modification was not accompanied by any consistent change in P_o nor did we observe the appearance of additional channels after the covalent reaction. Fig. 11 C contains the results of four similar experiments confirming the observation that covalent modification did not result in any consistent change in P_o. This result is consistent with the notion that the effects of covalent modification were largely, if not exclusively, due to a change in the single-channel conductance, rather than to a change in P_o or to a change in the number of channels in the plasma membrane (see Liu et al., 2001, in this issue).

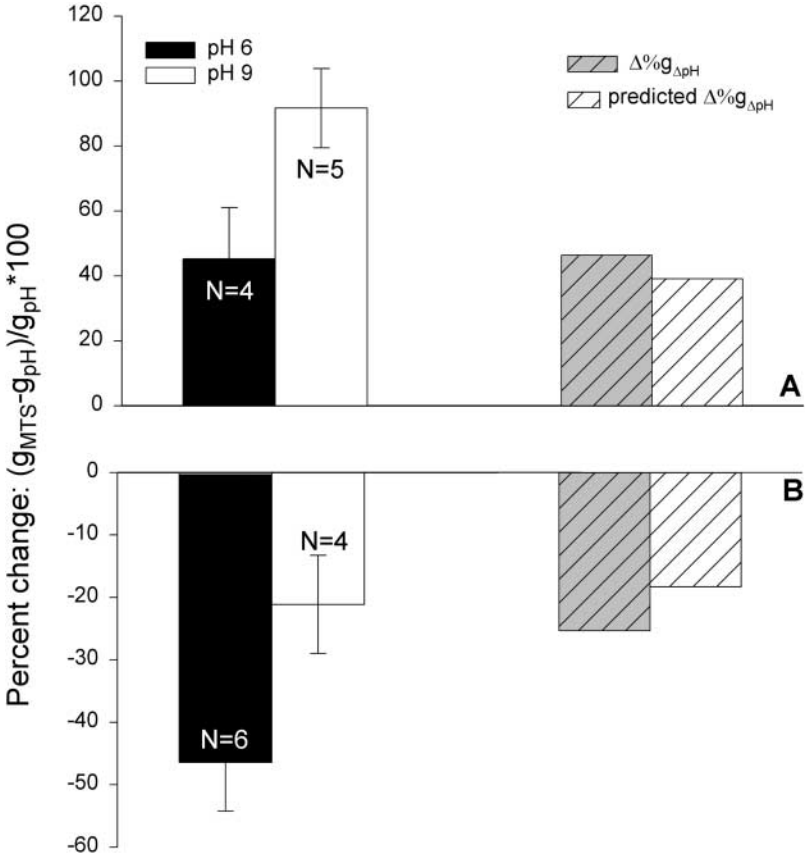

FIGURE 13. Functional effect of covalent modification of R334C CFTR was dependent on the bath pH. Shown is the percent change in oocyte conductance due to covalent modification at either pH 9.0 or pH 6, as described in RESULTS. Also shown is a comparison of the measured pH-dependent difference in the effects of MTSET and MTSES compared with that predicted on the basis of a pKa for the cysteine of 8.17 and the assumption that conductance was a linear function of the charge at this locus (see Fig. 18 B).

pH Titration of R334C CFTR Altered Both the Conductance and the Shape of the Current-Voltage Relation

The thiol moiety associated with a cysteine residue is expected to bear a time-average, partial negative charge, the magnitude of which will depend on the local pH and the pKa of the sulfhydryl group in situ. Thus, the charge associated with the cysteine at position 334 is expected to vary substantially with bath pH, and this offered the possibility of introducing graded changes in the time-average net charge at this site. The results presented in Fig. 12 A bear out this prediction. The conductance and the shape of the I-V relation of oocytes expressing R334C CFTR was highly dependent on the bath pH, exhibiting an apparent pKa of 8.17 ± 0.10 (n = 3; Fig. 12 B). This trend was consistent with the results obtained with covalent modification, i.e., acidification of the bath, a maneuver expected to decrease the probability of finding the sulfur in the ionized (negatively charged) state, increased conductance and reduced the inward rectification, whereas alkalinization of the bath had the opposite effect.

If the pH-dependent effects seen with R334C CFTR are due to graded changes in the time-averaged, partial negative charge associated the sulfhydryl group at the 334 locus, then the magnitude of the change induced by chemical modification of this locus should be dependent on bath pH. If the local pH is more alkaline than the pKa of the SH group, then the sulfur will bear a significant negative charge so that the total change in charge brought about by covalent modification will be the sum of that added by the deposition of the charged group and the pH-dependent component that is eliminated by the formation of the mixed disulfide bond. In contrast, if the pH is acidic with respect to the in situ pKa, then the total change in charge will approach that associated with the deposited group. Shown in Fig. 13 are the results of an experiment in which the effects of MTSET and MTSES on the conductance of oocytes expressing R334C CFTR were compared at a bath pH of 6.0 (solid bar) and pH 9.0 (open bar). The change in conductance seen with MTSET was greater at pH 9, as expected if the formation of the mixed disulfide bond eliminated the charge on the S at position 334. Likewise, the change seen with MTSES was reduced at alkaline pH, presumably because the covalent addition of negative charge was partially compensated by the elimination of the negative charge on the S. The hatched bars compare the observed difference in the effect of labeling at pH 6.0 and pH 9.0 with that predicted on the basis of the empirically determined pKa value of 8.17. The similarity of these values provides support for the proposition that the effects of bath pH changes and covalent labeling were both attributable to the SH group at position 334.

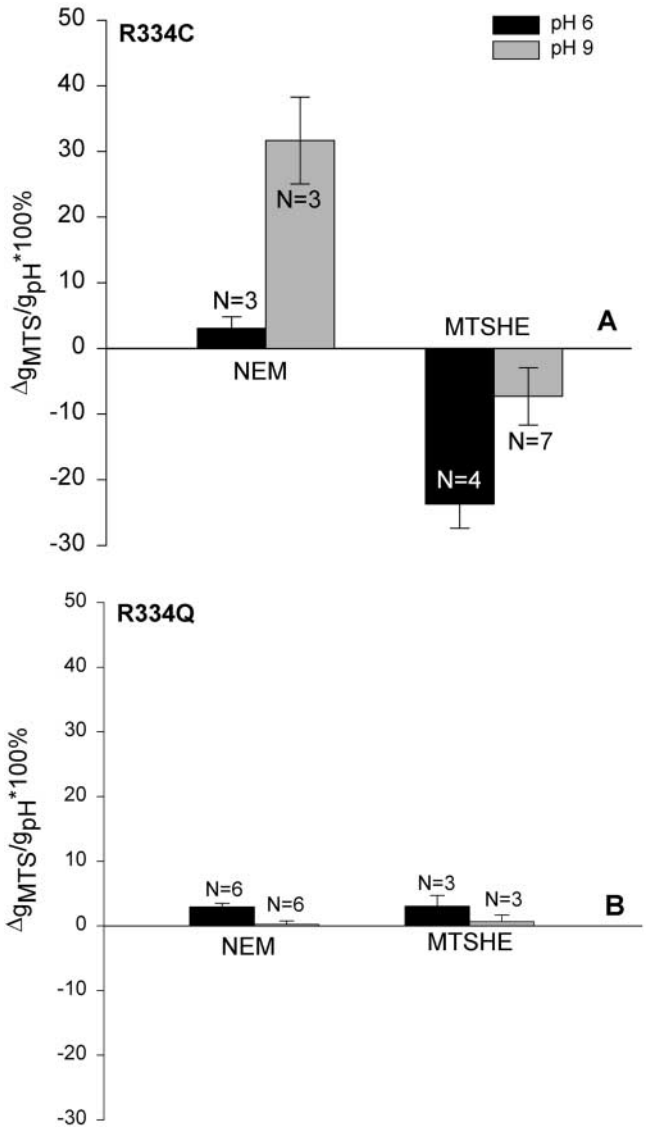

FIGURE 14. Modification of R334C CFTR with neutral reagents caused pH-dependent changes in conductance. (A) Change in conductance of oocytes expressing R334C CFTR when modified with either NEM or MTSHE at either pH 9.0 or pH 6. NEM behaved as expected for a neutral reagent whereas MTSHE, which is expected to be polar but uncharged, did not. (B) The results of similar experiments conducted using constructs in which the arginine at position 334 was replaced by a nonreactive amino acid (glutamine).

The effect of bath pH on the functional impact of covalent charge deposition at position 334, along with the effects of pH titration, per se, strongly suggested that charge changes could be affected by the addition of neutral moieties if the bath pH was such that the modification eliminated net negative charge on the cysteine. Shown in Fig. 14 are the results of modifying R334C CFTR with two "neutral" reagents, NEM and MTSHE. It can be seen that, in the presence of a bath pH of 9.0, exposure to NEM increased conductance, as expected if a negative charge at the site was eliminated. In contrast, at an acidic pH, NEM was without effect although it blocked covalent modification by MTSET (unpublished data). The conductance of oocytes expressing R334Q CFTR was independent of pH and was not greatly altered by NEM. Exposure of oocytes expressing R334C CFTR to MTSHE at acidic pH produced an effect reminiscent of MTSES, a conductance decrease, as if negative charge had been added. The effect was diminished at pH 9, as expected if, as with MTSES, there was a partial cancellation of charge added and charge eliminated due to labeling. This response may be attributable to the dipolar character of the terminal hydroxyl group of MTSHE or could reflect some other effect of this modification on the conformation of the protein. Exposure of oocytes expressing R334Q CFTR to MTSHE produced only small changes in conductance.

pH Titration of R334H CFTR Altered Conductance and the Shape of the I-V Relation

It was of interest to compare the response to changes in bath pH of R334C CFTR with that of R334H CFTR. The side chain of histidine is expected to bear a time-average, partial positive charge, the magnitude of which will depend on the local pH and the pKa of the imidazole group in situ. An I-V plot from a representative experiment in which the pH of the solution bathing an oocyte expressing R334H CFTR was acidified from 7.4 to 6.02 and then 4.80 is shown in Fig. 15 A. Acidification of the bath from pH 7.4 to 6.02 led to an immediate increase in conductance and slight reduction in the inward rectification. Further acidification to pH 4.80 led to an additional increase in conductance and a nearly linear current-voltage relation without shifting the reversal potential. The apparent pKa for the conductance change was 5.68 ± 0.08 ($n = 4$; Fig. 15 B).

Stepwise acidification of the bath led to stepwise increases in the conductance of oocytes expressing R334C or R334H CFTR and corresponding, stepwise increases in the rectification ratio, whereas similar pH changes resulted in only modest changes in the conductance of oocytes expressing wt CFTR. For example, a 3-min exposure of wt CFTR to pH 4.86 caused a 6% reduction in conductance and a 5% reduction in outward rectification. After 20 min, conductance had decreased by a total of 11%, but there was no further change in rectification. The observed changes seen with wt CFTR were opposite of those seen with oocytes expressing R334C or R334H CFTR, suggesting that the pH induced changes due to protonation of R334C or R334H were, if anything, slightly underestimated.

The distinct pKa's of the R334C and R334H variants favor the notion that these pH-dependent effects are due to titration of the side chain at position 334, as opposed to a mutation-induced exposure of a titratable site at another locus (Coulter et al., 1995). The appar-

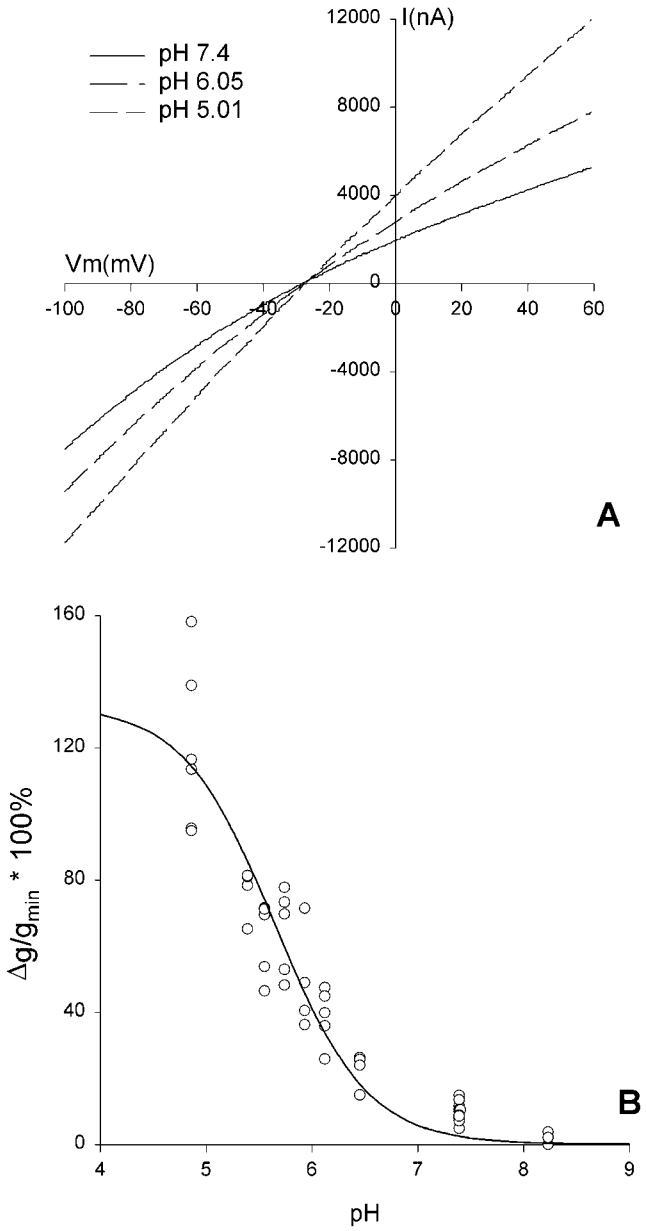

FIGURE 15. pH titration of oocytes expressing R334H CFTR altered both the conductance and the shape of the I-V relation. (A) I-V plots from an oocyte expressing R334H CFTR. After achieving steady-state activation in stimulatory cocktail at pH 7.4 (solid line), acidification of the bath to pH 6.0 (dotted line) or pH 4.8 (dashed line) increased conductance and deprecated inward rectification without altering the reversal potential. (B) Percent increase in conductance, normalized to the lowest conductance observed (most alkaline pH), plotted versus the bath pH for four different oocytes. Eq. 1 was fitted and resulted in a mean pKa of 5.68 ± 0.08 and a mean $\%g_{max}$ of 129 ± 15.5. The solid line represents the Henderson-Hasselbach equation for a pKa of 5.68.

ent pKa's agreed well with the values for the thiol group of cysteine (pKa 8.5) or the imidazole of histidine (pKa 6.5) in solution (Stryer, 1988, p. 21). The fact that both values were more acidic than those seen in solution might reflect the proximity of the positively charged lysine at position 335.

Amino Acid Substitutions for R334 and K335 Tended to Alter the Shape of the Macroscopic I-V Relation in a Charge-specific Fashion

Fig. 16 contains the results of experiments in which we compared the effects of point mutations on the shape of the macroscopic I-V relation. The rectification ratio is plotted as function of the charge at the R334 and K335 loci for variants in which the charge should be unchanged (K or R), fully or partially neutralized (Q, C, H, or A), or converted from positive to negative (E or D). The general trend among the panel of substitutions was consistent with the observations derived from chemical modification and pH titration. As the charge status at these loci varied from positive to negative, there was a shift in I-V shape from outward to inward rectification. However, for two mutants, R334H and K335A, the RR value clearly deviated significantly from that predicted by the general trend. It seems likely, particularly in view of the sensitivity of channel gating to amino acid substitution (Mansoura et al., 1998), that all of these amino acid changes altered channel structure, and it may be that the changes effected by the H and A substitutions differed significantly from the others in this group. Mutants might, for example, exhibit differential sensitivity to block by intracellular anions (Overholt et al., 1993, 1995; Linsdell and Hanrahan, 1996).

The Effects of Charge Deposition at Position 334 Were Consistent with the Predictions of Charged-vestibule Models for the Anion Conduction Path

The results of covalent modification and pH titration of R334C and R334H CFTR, as well as the functional impact of amino acid substitutions at this site, pointed to an important role for the charge at position 334 in determining the conduction properties of CFTR. Our analysis of the functional role of charges at this position was guided by several experimental results. First, charge changes at this locus produced correlated changes in macroscopic conductance and I-V shape. Second, single-channel recordings, although they were of necessity conducted under conditions that were very different from those used for the macroscopic measurements, revealed that positive charge addition increased single-channel conductance. Finally, P_o of single R334 CFTR channels was not altered by covalent modification nor was the increment in macroscopic conductance brought about by modification highly dependent on the activation state of the channel. To investigate the hypothesis that the coordinated changes in conductance and I-V shape seen with covalent modification of R334C CFTR could be attributed to a charge-induced change in the conduction properties of

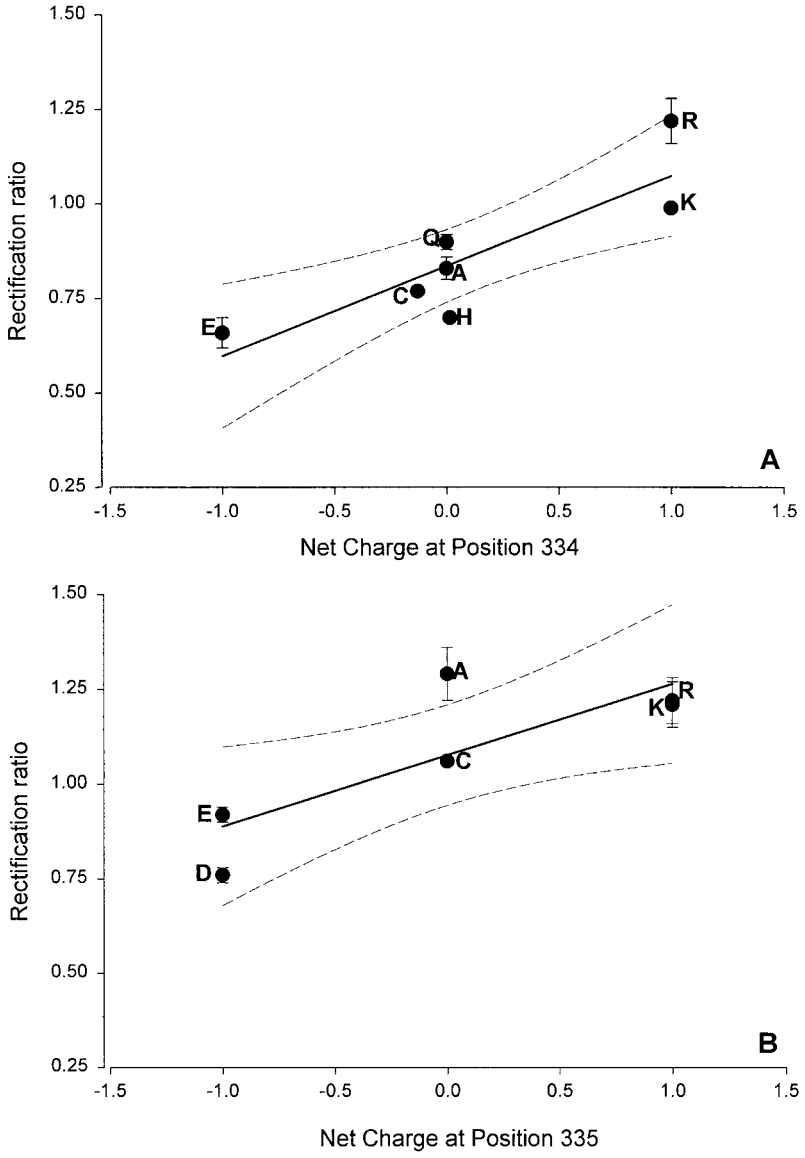

FIGURE 16. The shape of the I-V relation was correlated with the charge status of the amino acid substituted at positions 334 and 335. (A) RR, determined as described in MATERIALS AND METHODS, is plotted as a function of the net charge of the amino acid at position 334 at pH 7.4 where glutamic acid (E) is assigned a value of −1, cysteine (C) is assigned a value of −0.12 based on the apparent pKa of 8.17 for R334C CFTR, histidine (H), alanine (A), and glutamine (Q) are neutral, and lysine (K) and arginine (R) are assigned a value of +1. (B) RR is plotted as a function of the net charge of the amino acid at position 335 where glutamic acid (E) and aspartic acid (D) were assigned a value of −1, alanine (A) was treated as neutral, cysteine (C) was also treated as neutral because K335C CFTR exhibited a smaller pH responses and its apparent pKa was not determined, and lysine (K) and arginine (R) were assigned a value of +1. The charge status of H and C is dependent on the bath pH so the assignment of a neutral value in a bath pH of 7.4 introduces a slight error. Solid lines are least-squares fits and dashed lines are 95% confidence limits.

CFTR, we explored the predictions of a charged-vestibule model similar to that used by Lu and MacKinnon (1994) to analyze the electrostatic effects of pH titration of an engineered histidine in a K^+ channel. We modeled the channel as a narrow pore with wider, but shallower, vestibules at either end. Because the structure of CFTR is unknown, it was not possible to attach any physical dimensions to the vestibules so we envisioned them as comprising near equilibrium, buffer zones connecting the bulk solution and the rate-limiting region of the pore. The Cl concentration in each vestibule was related to that in the adjacent aqueous bath or cytoplasm by the Boltzmann equation (Eq. 2), i.e.,

$$\frac{[Cl]_o}{[Cl]_b} = e^{-\left(\frac{zF\Psi_o}{RT}\right)} \quad \text{and} \quad \frac{[Cl]_i}{[Cl]_c} = e^{-\left(\frac{zF\Psi_i}{RT}\right)}, \qquad (2)$$

where $[Cl]_o$, $[Cl]_b$, $[Cl]_i$, and $[Cl]_c$ represent, respectively, the chloride concentrations in the outer vestibule, the external bath, the inner vestibule, and the cell interior; and Ψ_o and Ψ_i, are the electrical potentials of the outer and inner vestibules measured with respect to the external bath and the cell interior, respectively. The vestibules were assumed to exhibit zero resistance to anion flow and each was characterized by a single, average electrical potential.

We compared two approaches to depicting the movement of chloride through the narrow region of the pore, a continuum model based on the Goldman equation (Goldman, 1943) and a rate-theory model like those previously used by Overholt et al. (1993, 1995) and Linsdell et al. (1997) to model CFTR. The former has the advantage of simplicity, but fails to account explicitly for anion binding within the pore. The latter in-

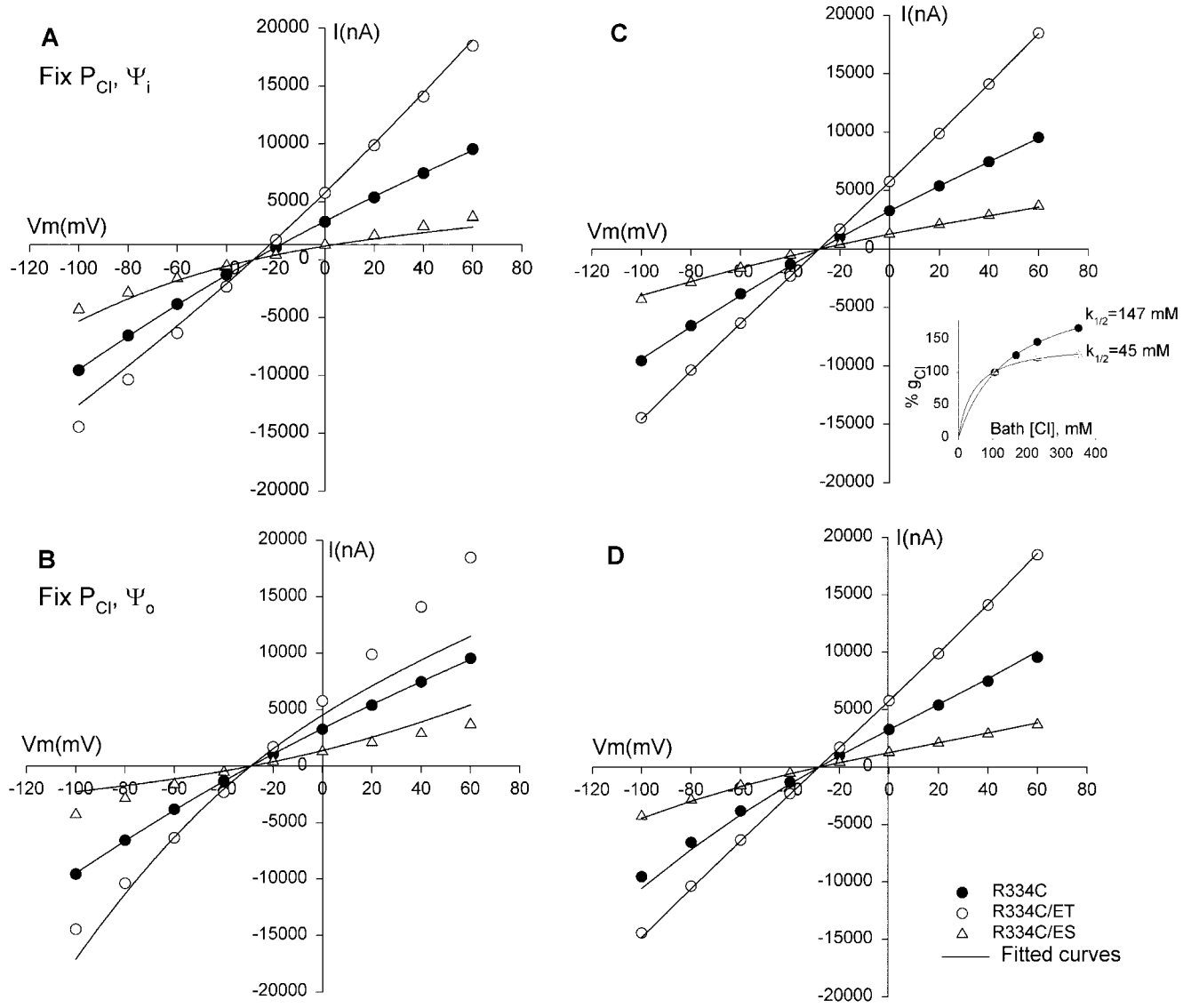

FIGURE 17. The effects of covalent modification of R334C CFTR could be simulated using charged vestibule models (see APPENDIX). The data points shown are the same as in Fig. 7 D containing unmodified R334C CFTR (closed circles), MTSET-modified R334C (open circles), and MTSES-modified R334C (closed triangles). (A) Continuum model with P_{Cl} and Ψ_i fixed, allowing Ψ_o to vary ($r^2 = 0.993$ for MTSET and 0.958 for MTSES). (B) Continuum model with P_{Cl} and Ψ_o fixed, allowing Ψ_i to vary ($r^2 = 0.879$ for MTSET and 0.826 for MTSES). (C) 4-barrier, 3-well rate-theory model simulating a high affinity channel, apparent $K_{1/2} = 38$ mM. Barriers (RT) = 3.65, 5.7, 6, and 7.1; wells (RT) = −0.7, −2.8, and −2. (closed circles) Unmodified R334C CFTR, $\Psi_o = 0$. (open circles) MTSET-modified R334C CFTR, $\Psi_o = +50$ mV. (closed triangles) MTSES-modified R334C CFTR, $\Psi_o = -10$ mV. (D) 4-barrier, 3-well rate-theory model simulating a low affinity channel, apparent $K_{1/2} = 115$ mM. Barriers (RT) = 3.8, 6, 7.5, and 7; wells (RT) = −0.1, −1.85, and −0.5. Symbols as in C for unmodified R334C CFTR ($\Psi_o = 0$), MTSET-modified R334C CFTR ($\Psi_o = +50$ mV), and MTSES-modified R334C CFTR ($\Psi_o = -10$ mV). (inset) Plots of percent increase ($\Delta g/g_{initial} \times 100\%$) in macroscopic CFTR conductance as function of bath Cl concentration for wt CFTR (open triangles) and unmodified R334C CFTR (closed circles).

cludes energy wells that represent binding sites for anions, but has the disadvantage of requiring a large number of adjustable parameters. We found that the effects of charge changes at position 334 could be simulated using either model, but that the estimated changes in vestibule potential due to charge changes was highly model-dependent. Representative examples of the results of both approaches are shown in Fig. 17.

Combining the Goldman equation with the equilibrium boundary conditions (see APPENDIX) yields, for the chloride current, I_{Cl}:

$$I_{Cl} = \frac{F^2}{RT} P_{Cl}(V_m + \Psi_i - \Psi_o) e^{\frac{F\Psi_o}{RT}} \left(\frac{[Cl]_b - [Cl]_c e^{\frac{-F\Psi_m}{RT}}}{1 - e^{\frac{-F}{RT}(V_m + \Psi_i - \Psi_o)}} \right), \quad (3)$$

where V_m is the measured transmembrane potential, and P_{Cl} is the chloride permeability of the narrow region of the pore.

An examination of Eq. 3 reveals that within the continuum model there are potentially five variables that might be adjusted to optimize the fit to the macroscopic I-V data: the chloride permeability (P_{Cl}), the potentials of the outer and inner vestibules (Ψ_o and Ψ_i), and bath and intracellular chloride concentrations ($[Cl]_b$ and $[Cl]_c$). Fits to I-V plots from representative experiments in which charge changes were accomplished by covalent labeling or pH titration were generated by starting with the most unbiased fit in which all parameters except the bath and intracellular chloride concentration were permitted to vary, and then exploring the effect of constraining one or more of the remaining parameters (in the course of such comparisons it was found that in all cases the intracellular concentration of chloride was set by the best fit to 34 mM so that this value was fixed and used for all subsequent computations).

The I-V shape characteristic of unmodified R334C CFTR at pH 7.4 was simulated by adjusting the values of Ψ_i and Ψ_o, but these values must be viewed as arbitrary for at least two reasons. First, the lack of structural information about CFTR and the simplicity of the model preclude a comprehensive analysis of all of the factors that might be expected to influence the absolute value of the vestibule potentials. Second, the calculated values are not independent of the initial choice for the value for permeability used to initiate the fitting process. We chose the initial value for P_{Cl} based on an estimate of permeability derived from a simple electrodiffusion analysis of the conductance measured at E_{rev}. For example, a conductance ($@E_{rev}$) of 100 μS was equated with a permeability of 4.09×10^{-7} cm^3/s using the relation $g_{Cl} = (F^2/RT)P_{Cl}\{([Cl]_o + [Cl]_i)/2\}$ (Dawson, 1996). Based on the initial best fit to the data for unmodified R334C CFTR, P_{Cl} was fixed at 3.4×10^{-7} cm^3/s, and the premodification values of Ψ_i and Ψ_o were set at +33 mV and −9 mV, respectively. When these parameters were used to fit the data for covalently modified R334C CFTR, the effect of MTSET (P_{Cl}, Ψ_i fixed) was attributed to a 24-mV increase in Ψ_o and that of MTSES to a 39 mV reduction of Ψ_o (Fig. 17 A). We explored a variety of ways of simulating the macroscopic I-V plots in which values for P_{Cl}, Ψ_o, and Ψ_i and were fixed or held constant in various combinations. The changes in the I-V plots induced by covalent modification could only be fit if Ψ_o was permitted to vary. For example Fig. 17 B shows the results obtained if P_{Cl} and Ψ_o were held constant and only Ψ_i was permitted to vary. In addition, using different starting values for P_{Cl}, Ψ_i, and Ψ_o yielded similar values for the change in Ψ_o induced by MTSET or MTSES (unpublished data). Titration of R334C and R334H CFTR by varying bath pH was also well described by a continuum model in which the changes in conductance and I-V shape were largely attributed to changes in Ψ_o (unpublished data).

Anion binding might be expected to attenuate the effects of increased chloride concentration in the outer vestibule on pore conductance if the rate of anionic flux were approaching saturation. To determine if saturation of anion flow rate might impact the conductance of R334C CFTR we compared the effects on oocyte conductance of raising the Cl concentration in the external bath. The inset to Fig. 17 summarizes the results of several experiments in which bath Cl was raised in steps from 105 to 350 mM. In each case, after steady-state activation had been achieved, the oocyte was exposed to an increased salt concentration for ~1 min and returned to the 105 mM bath. The maximum change in the background conductance evoked in noninjected oocytes by the same maneuvers was, at most, 3% of that seen in CFTR expressing oocytes and was ignored in this analysis. In oocytes expressing wt CFTR, the maximum conductance increase averaged ~25% and the points could be fit by a rectangular hyperbola having an apparent $K_{1/2}$ of 45 mM. In contrast, the maximum increase in conductance in oocytes expressing R334C CFTR (unmodified) was ~70% at 350 mM and consistent with an apparent $K_{1/2}$ of 147 mM, in accord with the notion that Cl binds in the pore of the R334C CFTR, but with lower affinity than that seen with wt CFTR. We refer to the $K_{1/2}$ values as "apparent" in as much as they were measured by raising Cl concentration on the outside solution only, and because we cannot distinguish concentration-dependent changes in anion binding from possible effects of ionic strength due to charge screening (Green and Andersen, 1991).

Fig. 17 (C and D) contains the results of interpreting the results of charge-change experiments using rate-theory models in which the binding of anions within the pore was simulated by placing energy wells within the conduction path. We used a 4-barrier, 3-well model for the pore as this configuration had been used previously by Linsdell et al. (1997) to simulate anion binding in CFTR. Initially, values of Ψ_o and Ψ_i were set to zero, the relative heights (see Fig. 17 legend) of equally spaced barriers and wells (without ionic repulsion) were chosen to reproduce the inward rectifying shape of the I-V curve for unmodified R334C CFTR. The barrier heights were scaled to achieve a single-channel conductance of ~0.5 pS, and the macroscopic current was scaled according to the measured current at $V_m = 0$. Single-channel conductance in the presence of symmetric high salt was 1.2 pS (Fig. 10), so we used 0.5 pS as an estimate for the conditions pertaining to the two-electrode measurements. We used two sets of energy values: one chosen to simulate a "low affinity" channel ($K_{1/2}$ = 115 mM) like R334C CFTR; and the other chosen to simulate a "high

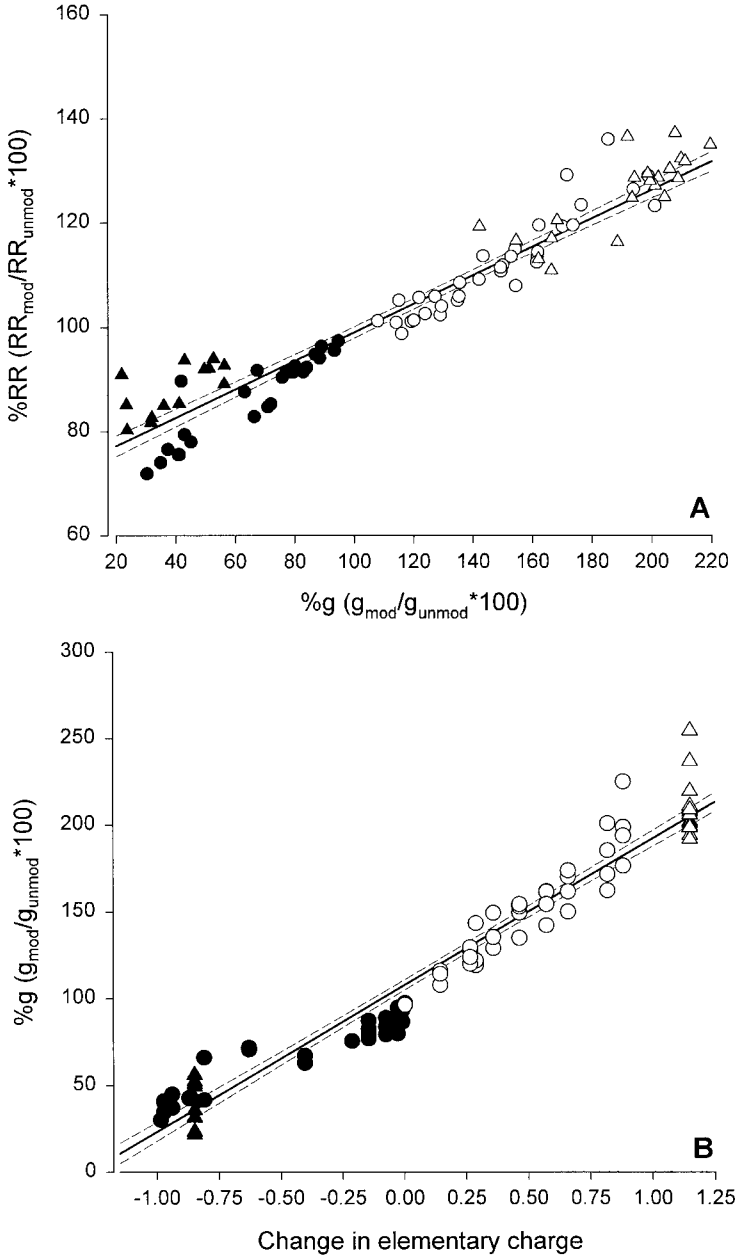

FIGURE 18. (A) The fractional changes in conductance and rectification ratio were correlated. Data points include charge changes brought about by thiol modification of R334C CFTR with positively charged reagents (open triangles), and negatively charged reagents (closed triangles), pH titration of R334C CFTR (closed circles), and pH titration of R334H CFTR (open circles). The solid line is the least-squares fit to the data. (B) Fractional change in conductance plotted versus the fractional change in elementary charge at position 334. Thiol modification of R334C CFTR with positively charged reagents (open triangles) was treated as adding a single positive charge; thiol modification of R334C with negatively charged reagents (closed triangles) was treated as adding a single negative charge; pH titration of R334H CFTR (open circles) was treated as adding a time-average positive charge determined by the bath pH, assuming a pKa of 5.68; and pH titration of R334C CFTR (closed circles) was treated as adding a time-average negative charge determined by the bath pH assuming a pKa of 8.17. Solid line is least-squares fit to the data, dashed lines are 95% confidence limits.

affinity" channel ($K_{1/2}$ = 38 mM) like wt CFTR. The values were chosen so that the "affinity" of the channel for Cl would be, if anything, somewhat higher than that observed (Fig. 17, inset) and, therefore, likely to highlight the impact of anion binding. It can be seen that the effects of modification by MTSET or MTSES could be simulated using either energy profile, with identical values for Ψ_o. Simulating the effect of positive charge addition required an increase in Ψ_o of +50 mV, whereas negative charge addition was simulated by a negative potential of −10 mV. This asymmetry is consistent with the fact that within the rate-theory formalism, the addition of a negative surface charge not only reduces the vestibule concentration of Cl, but also creates a component of the intramembrane electric field that will tend to destabilize anion binding (reduced well depth), whereas the addition of positive charge, although it increases local Cl concentration, also adds an electric field component that tends to stabilize anion binding by deepening the wells (MacKinnon et al., 1989). Hence, the effects of modification by MTSET or MTSES could be simulated using either a continuum or a rate-theory approach, but the values of Ψ_o required by the rate-theory model differed significantly from those estimated from the diffusion model.

Fig. 18 A summarizes the data from experiments in which charge changes were effected in R334C and R334H CFTR by means of chemical modification or pH titration. Plotted are values calculated for the percent change in conductance and RR from the unmodified

state for MTSET and MTSES and percent change from the value seen at pH 7.4 for the pH titration experiments. It can be seen that there is a consistent correlation between changes in RR and conductance brought about by charge changes at position 334. Although we do not know the actual values of the vestibule potential, we can estimate the change in elementary charge associated with thiol modification or pH titration. Fig. 18 B is a plot of the fractional change in conductance versus the fractional change in elementary charge at residue 334. The points representing covalent modification of R334C by MTSET or MTSES were corrected for a small (14.5%) charge change predicted due to the protonation state of the cysteine at pH 7.4. Simulations (Fig. 17) suggest that a change in elementary charge from negative one to positive one is associated with a change in vestibule potential of the order of 20–60 mV, which are values within the range predicted by Dani (1986) to result from a single charge placed in a vestibule. The linear relation between the change in conductance and the change in elementary charge is consistent with a model in which the vestibule potential is an approximately linear function of vestibule charge, as suggested by Dani's Fig. 5 and the "capacitor approximation" for the double layer potential at low voltages (Dani, 1986). The observed parallel change in g_{Cl} and RR provides support for the hypothesis that charge changes at position 334 modulate Cl movement, at least in part, by altering the local electrostatic potential.

DISCUSSION

Accessibility of Charged Sites in TM 6

The results presented here demonstrate a clear difference in the accessibility to impermeant MTS reagents of sites in TM6 that are normally occupied by charged residues. The outermost sites (based on an ideal helical representation of TM 6) that are normally occupied by R334 and K335 are readily accessible from the external bath, whereas the innermost sites, normally occupied by R347 and R352, are not. Even if we allow for the possibility of some modest accessibility of R352C, it is evident that the outer sites are highly reactive, whereas the inner sites are either not at all reactive or much less so. As indicated, this finding is at variance with published results. The source of the discrepancy is not immediately clear, but might be related to the fact that previous investigations generally relied on measurements of the Cl current at a fixed potential of −100 mV as a measure of efficacy rather than on the conductance as determined in the present study. The former parameter is more vulnerable to errors due to shift in reversal potential, the electrode potential, or simply a decline in the health of the oocyte. It must be understood that the negative finding could reflect, not only failure of the reagents to reach or react with the engineered cysteine, but also failure of the reaction to occur due to some conformational constraint. In addition, we cannot eliminate the possibility that a reaction occurred, but was without functional impact.

The results of control mutations, and the convergence of results obtained using covalent modification, pH titration, and amino acid substitution, all support the conclusion that the functional effects of these maneuvers can be localized to the sites where R334 and K335 reside in the wild type protein. This is an important point because in the course of our experiments (e.g., R352C CFTR) and those of others using cysteine accessibility or pH titration (Coulter et al., 1995; Akabas, 1998), it has become apparent that structural changes can render sites "distant" from the mutation accessible or titratable. The evidence for a single site of action of thiol reagents and protons is particularly strong for R334C CFTR as we were able to demonstrate a pH-dependent modulation of functional effects of covalent modification.

The Charge Present at R334 Is a Critical Determinant of CFTR Function: Does this Charge Lie within the Pore?

The functional effects of altering the charge at residue 334 exhibited a consistent pattern. Experimental maneuvers that rendered the charge at the site more positive increased macroscopic conductance and also increased the rectification ratio, whereas maneuvers that increased negative charge at this site had the opposite effect. It was particularly striking that the effects of covalent addition of charged groups were similar to those seen with simply adding or removing protons. It was also apparent that even neutral reagents can alter local charge by eliminating the pH-dependent charge on the engineered cysteine. The relatively low single-channel conductance seen with R334C CFTR (even at elevated Cl concentrations) before modification with MTSET and in the patient mutation R3334W (Sheppard et al., 1993) is consistent with the hypothesis that R334 is an important determinant of pore conductance. The fact that modification with MTSET raised the single-channel conductance confirmed, in part, the prediction based on macroscopic conductance. However, differences in the experimental conditions made a detailed quantitative comparison of the two measurements impossible. It seems reasonable to conclude that the charge at this site is an important determinant of channel function, and although we speculate that R334 may lie in the pore (as discussed in the next section), it is important to note that covalent addition of a positively charged moiety to R334C CFTR (MTSET) did not rescue the wild-type phenotype. The single-channel conductance of 3.7 pS seen after MTSET modification of R334C was less than half of that seen with wt CFTR (8.6

pS) in the same experimental setting. Thus, the substitution of cysteine for the native arginine may have altered the structure of the protein in a way that was not corrected by simply replacing the positive charge. Three patient mutations at this site are listed in the Cystic Fibrosis Foundation Mutation database. One of these, R334W, was studied by Sheppard et al. (1993) who reported that single-channel currents were undetectable in patches detached from HeLa cells in symmetric Cl of ~160 mM, which is consistent with the reduced conductance reported here for R334C CFTR.

A Charged-vestibule Model

The results presented here are consistent with the hypothesis that R334 (and perhaps K335) lies within the outer vestibule of the anion-conducting pore of the CFTR Cl channel. The essence of the charged vestibule model was well described by Green and Andersen (1991) who envisioned the general features of channel structure as an evolutionary solution to the limitation on conduction rate that is imposed by diffusion. They reviewed theoretical and experimental results, all of which suggest that rapid ion translocation across the thickness of a biological membrane is only possible if the "narrow" region of the pore, presumably responsible for selectivity and binding, is flanked by vestibules designed not only to increase the "capture radius" at the channel mouth, but also to concentrate permeant ions by electrostatic means. The results presented here are consistent with a scheme in which R334 is placed within the outer vestibule of the CFTR Cl channel where its charge acts to promote the accumulation of Cl and thereby to create "a conditioned environment" adjacent to the rate-limiting section of the pore (Dani, 1986).

The charged-vestibule model provides a relatively straightforward explanation for a consistent finding in these experiments, namely that charge changes at position 334 produced highly correlated changes in conductance and I-V shape, such that increasing positivity increased anion conductance and altered shape from inwardly rectifying toward linearity. The charged-vestibule model attributes both the change in conductance and the change in I-V shape to the increase in the time-average concentration of the permeant anion in the vestibule, adjacent to the rate-limiting segment of the pore. Conductance, determined around E_{rev}, is increased because the time-average occupancy of this pore region by anions is increased. The change in I-V shape results because increased local external concentration of Cl favors outward current (inward anion flow) as V_m becomes positive with respect to E_{rev}. Identical changes in conductance and rectification are predicted to result from simply raising the concentration of the permeant anion in the external bath, as long as the increase in ionic strength does not alter the vestibule potential. An increase in bath concentration imposed across an ion-selective channel creates an additional component of the electric field within the membrane that is sensed as a change in the reversal potential. In contrast, turning on a charge in the vestibule creates a local potential near the outer surface of the membrane that obligates an increase in vestibule anion concentration and also creates an additional component of the intramembrane field. In the near-equilibrium situation, these effects cancel so that there is no change in reversal potential.

We cannot exclude the possibility that charge changes at position 334 can influence the properties of the channel in ways that are not captured in the charged-vestibule model. Although single-channel conductance is clearly modified by covalent charge changes, there may be changes in channel gating and in the properties of the permeation path that were not discerned here. For example, charge-dependent changes in voltage-dependent block of CFTR by some intracellular constituent could, in principle, contribute to changes in I-V shape. Overholt et al. (1993, 1995) and Linsdell et al. (1997; see also Linsdell and Hanrahan, 1996) reported that exposure of the cytoplasmic side of detached patches to gluconate and glutamate produced voltage-dependent block of CFTR and an outwardly rectifying I-V relation. If we assume that the outward rectification seen with wt CFTR is due in part to block of Cl efflux by intracellular anions, then the inward rectification seen with R334C CFTR could be attributed, in part, to a reduction in this blocking effect in the mutant channel. In fact, such changes are predicted by rate-theory simulations (see RESULTS) and are due to the effect of the charge-dependent change in the intra-membrane field on well depth (see RESULTS). The changes in I-V shape brought about by charge changes at R334 would in this scheme be attributed to a partial restoration of block (MTSET, acidic pH) or a further reduction of block (MTSES, basic pH). We cannot exclude some contribution of changes in voltage-dependent block to the results presented here, but this mechanism cannot be the sole basis for the charge-induced effects on anion conduction in as much as MTSET, for example, reduced inward rectification, but also substantially increased conductance.

Implications for Pore Structure and Electrostatics

It must be emphasized that the absence of a structure for the pore domain precludes any conclusions about the actual value of ψ_o, which is the total average potential that we assign to the outer vestibule. In other words, positive charges at positions 334 and 335 may make the vestibule potential positive with respect to the extracellular solution or they may simply act to wholly or partially overcome a negative potential produced by

other charged or polar entities that make up the outer vestibule. It was also clear that estimates for the changes in Ψ_o brought about by covalent modification were dependent on the assumptions used to model the conduction path. In any case the charges at these positions appear likely to be important determinants of the conductance of the CFTR pore.

The phenotype that we have used here to tentatively assign R334 to the pore of CFTR has a counterpart in cation-selective channels. Pascual et al. (1995) studied the effects of externally applied MTS reagents on Kv2.1 channels and noted a charge-dependent effect on cation conduction, but reported dramatically different effects of covalent labeling of cysteines substituted for adjacent residues, I379 and Y380. The conductance of oocytes expressing the I379C construct was reduced by MTS reagents (MTSET, MTSEA, and MTSES) regardless of charge, whereas the effects of the same reagents on oocytes expressing the Y380C construct were distinctly charge-dependent. The anionic reagent (MTSES) increased the macroscopic conductance of oocytes expressing Y380C and altered the shape of the I-V plot from outwardly rectifying to nearly linear, whereas cationic reagents (MTSET and MTSEA) reduced the conductance and enhanced the rectification, exactly as predicted for a residue that resides near the mouth of a cation-selective pore. Single-channel records disclosed that MTS reagents altered the unitary conductance of Y380C channels as would be predicted from macroscopic records, but did not affect channel gating. It is now possible to suggest an explanation for the differences in the behavior of these two adjacent residues based on the crystal structure subsequently determined for the bacterial channel, Kcsa (Doyle et al., 1998). The structure shows the Kcsa residue most likely analogous to Y380 of Kv2.1 (Y82) protruding directly into the mouth of the pore where a charge would be likely to influence the concentration of K immediately adjacent to the signature GYG sequence that forms the selectivity filter of the channel. The adjacent residue (L81), which is analogous to I379 of Kv2.1, is predicted by the structure to be oriented away from the mouth of the pore. Yang et al. (1995) studied the oxidation of I379C in Kv2.1 by H_2O_2. They found that treatment reduced the probability of opening of Kv2.1 channels, but did not alter the unitary currents. In addition, it was possible to form a disulfide linkage between a cysteine located at position 379 and an endogenous cysteine in a neighboring transmembrane segment at position 394. Taken together, these results suggest that this residue, although it adjacent to Y380, plays a very different role in the structure and function of the protein. A residue analogous to Y380 in Kv2.1 has also been studied in the *Shaker* K channel (Liu et al., 1996) and modification produced dramatic effects on C-type inactivation that were not highly charge dependent. Thus, modification of a single residue could easily lead to significant effects on both conduction and gating. Amino substitutions in the acetylcholine receptor channel altered cation conductance in a charge-dependent fashion (Imoto et al., 1988), but Kienker et al. (1994) concluded that the impact of charge substitutions on channel function could not be reconciled with a simple, surface charge model. Thus, we would propose that charge-dependent effects such as those reported here may be a useful first approach to defining the conduction path of the CFTR, but that in the absence of structural information any such analysis must be applied with caution.

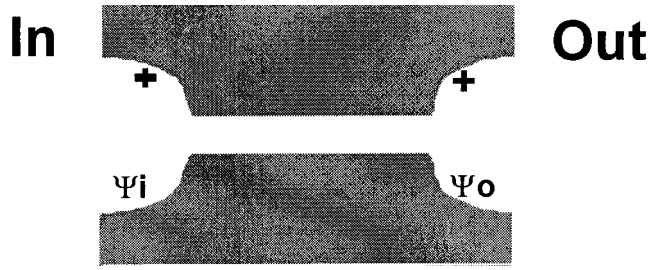

FIGURE 19. Cartoon illustrating the features of the charged vestibule model.

APPENDIX

A Charged Vestibule Pore Continuum Model

The anion conduction pathway is envisioned as a narrow pore flanked by two wide and relatively shallow vestibules, such that the resistance to anion conduction resides solely in the narrow pore (Fig. 19).

Each vestibule is assumed to contain net charge, shown here as positive. The flow of chloride through the narrow pore was modeled using the Nernst-Planck equation with the assumption of a constant electric field (Goldman, 1943):

$$I_{Cl} = \frac{F^2}{RT} P_{Cl} V_m \left(\frac{[Cl]_o - [Cl]_i \, e^{\frac{-FV_m}{RT}}}{1 - e^{\frac{-FV_m}{RT}}} \right), \qquad \text{(A1)}$$

where I_{Cl} is the Cl current, P_{Cl} is the Cl permeability, V is the transmembrane potential, $[Cl]_o$ is the Cl concentration in the outer vestibule, $[Cl]_i$ is the Cl concentration in the inner vestibule, and F, R and T have their usual meaning.

The concentration of Cl within the outer vestibule of the channel, $[Cl]_o$, is assumed to be in equilibrium with that in the bath, $[Cl]_b$, as specified by the equality of the Cl electrochemical potentials in the two regions:

$$\mu^o_{Cl} + RT\ln[Cl]_o + zF\Psi_o = \mu^b_{Cl} + RT\ln[Cl]_b + zF\Psi_b, \qquad \text{(A2)}$$

where μ^o_{Cl} and μ^b_{Cl} are, respectively, the standard chemical potentials for Cl in the outer vestibule and the aqueous bath, and Ψ_o and Ψ_b are the electrical potentials in the outer vestibule and the bath. Setting $\mu^o_{Cl} = \mu^b_{Cl}$ and $\Psi_b = 0$ and solving Eq. A2 for $[Cl]_o/[Cl]_b$, we obtain:

$$\frac{[Cl]_o}{[Cl]_b} = e^{-\left(\frac{zF\Psi_o}{RT}\right)}. \quad \text{(A3)}$$

Likewise, for the inner vestibule we have:

$$\frac{[Cl]_i}{[Cl]_c} = e^{-\left(\frac{zF\Psi_i}{RT}\right)}, \quad \text{(A4)}$$

where Ψ_i is the electrical potential of the inner vestibule with respect to that of the cell interior and $[Cl]_c$ is the cytoplasmic Cl concentration. In describing these equilibria, we assumed that the standard chemical potential for chloride is identical in the bath, the cell interior and in the inner and outer vestibules. This is equivalent to the assumption that the vestibule is sufficiently large that chloride is solvated essentially as it would be in aqueous solution, and that the reduced dielectric constant estimated by Smith et al. (1999) pertains to the narrow pore region of the pore and its influence is lumped into the value of P_{Cl}.

Substituting Eqs. A3 and A4 into Eq. A1, yields:

$$I_{Cl} = \frac{F^2}{RT} P_{Cl}(V_m + \Psi_i - \Psi_o) e^{\frac{F\Psi_o}{RT}} \left(\frac{[Cl]_b - [Cl]_c e^{\frac{-FV_m}{RT}}}{1 - e^{\frac{-F}{RT}(V_m + \Psi_i - \Psi_o)}} \right), \quad \text{(A5)}$$

where Ψ_i is the total potential within the internal vestibule, Ψ_o is the total potential within the external vestibule and $[Cl]_b$ and $[Cl]_c$ are the bath and cytoplasmic Cl concentrations, respectively.

Examination of the term in brackets in Eq. A5 reveals that the reversal potential is independent of Ψ_i and Ψ_o. This is a result of approximating the distribution of anions between the vestibules and the solutions that bath them as an equilibrium. Regardless of the values of the vestibule potentials, the interfaces remain at equilibrium so that the reversal potential is constant. This assumption, common in channel models (Dani, 1986; Lu and MacKinnon, 1994; MacKinnon et al., 1989; MacKinnon and Miller, 1989), assigns the "rate-limiting step" in anion translocation to a narrow, interior region of the pore.

We would like to thank M. Akabas, R. Joho, and H. Lester for supplying constructs used in these studies, T. Amano, J. Billingsley, A.L. Burtch, S. Yukl, and E. Pratt for assistance with the experiments, and M. Mansoura, T. Begenisich, and E. McClesky for assistance with rate-theory models.

This work was supported by grants to DCD from the National Institutes of Health (No. DK45880), the University of Michigan Gut Peptide Center, and the Center for Membrane Toxicology Study at the Mount Desert Island Biological Laboratory and a grant to N.A. McCarty from the Cystic Fibrosis Foundation (MCCART00P0). During a portion of this work, X. Liu was supported by the Cystic Fibrosis Foundation.

Submitted: 30 July 2001
Revised: 30 July 2001
Accepted: 27 August 2001

REFERENCES

Akabas, M.H. 1998. Channel-lining residues in the M3 membrane-spanning segment of the cystic fibrosis transmembrane conductance regulator. *Biochemistry.* 37:12233–12240.

Akabas, M.H., C. Kaufmann, T.A. Cook, and P. Archdeacon. 1994. Amino acid residues lining the chloride channel of the cystic fibrosis transmembrane conductance regulator. *J. Biol. Chem.* 269: 14865–14868.

Anderson, M.P., R.J. Gregory, S. Thompson, D.W. Souza, S. Paul, R.C. Mulligan, A.E. Smith, and M.J. Welsh. 1991. Demonstration that CFTR is a chloride channel by alteration of its anion selectivity. *Science.* 253:202–205.

Baumgartner, W., L. Islas, and F.J. Sigworth. 1999. Two-microelectrode voltage clamp of Xenopus oocytes: voltage errors and compensation for local current flow. *Biophys. J.* 77:1980–1991.

Begenisich, T.B., and M.D. Cahalan. 1980. Sodium channel permeation in squid axons. II: Non-independence and current-voltage relations. *J. Physiol.* 307:243–257.

Cheung, M., and M.H. Akabas. 1996. Identification of cystic fibrosis transmembrane conductance regulator channel-lining residues in and flanking the M6 membrane-spanning segment. *Biophys. J.* 70:2688–2695.

Cheung, M., and M.H. Akabas. 1997. Locating the anion-selectivity filter of the cystic fibrosis transmembrane conductance regulator (CFTR) chloride channel. *J. Gen. Physiol.* 109:289–299.

Cotten, J.F., and M.J. Welsh. 1999. Cystic fibrosis-associated mutations at arginine 347 alter the pore architecture of CFTR: evidence for disruption of a salt bridge. *J. Biol. Chem.* 274:5429–5435.

Coulter, K.L., F. Perier, C.M. Radeke, and C.A. Vandenberg. 1995. Identification and molecular localization of a pH-sensing domain for the inward rectifier potassium channel HIR. *Neuron.* 15: 1157–1168.

Dani, J.A. 1986. Ion-channel entrances influence permeation. Net charge, size, shape, and binding considerations. *Biophys. J.* 49: 607–618.

Dawson, D.C. 1996. Permeability and conductance in ion channels: a primer. *In* Molecular Biology of Membrane Transport Disorders. T.F. Andreoli, J.F. Hoffman, D.D. Fanestil, and S.G. Schultz, editors. Plenum Press, New York. 87–109.

Dawson, D.C., S.S. Smith, and M.K. Mansoura. 1999. CFTR: mechanism of anion conduction. *Physiol. Rev.* 79:S47–S75.

Doyle, D.A., J.M. Cabral, R.A. Pfuetzner, A. Kuo, J.M. Gulbis, S.L. Cohen, B.T. Chait, and R. MacKinnon. 1998. The structure of the potassium channel: molecular basis of K^+ conduction and selectivity. *Science.* 280:69–77.

Drumm, M.L., D.J. Wilkinson, L.S. Smit, R.T. Worrell, T.V. Strong, R. Frizzell, D.C. Dawson, and F.S. Collins. 1991. Chloride conductance expressed by delta F508 and other mutant CFTRs in *Xenopus* oocytes. *Science.* 254:1797–1799.

Fraser, C.M. 1989. Site-directed mutagenesis of beta-adrenergic receptors. Identification of conserved cysteine residues that independently affect ligand binding and receptor activation. *J. Biol. Chem.* 264:9266–9270.

Goldin, A.L. 1992. Maintenance of *Xenopus laevis* and oocyte injec-

tion. *Methods Enzymol.* 207:266–279.

Goldman, D.E. 1943. Potential, impedance, and rectification in membranes. *J. Gen. Physiol.* 27:37–60.

Green, W.N., and O.S. Andersen. 1991. Surface charges and ion channel function. *Annu. Rev. Physiol.* 53:341–359.

Guinamard, R., and M.H. Akabas. 1999. Arg352 is a major determinant of charge selectivity in the cystic fibrosis transmembrane conductance regulator chloride channel. *Biochemistry.* 38:5528–5537.

Holmgren, M., Y. Liu, Y. Xu, and G. Yellen. 1996. On the use of thiol-modifying agents to determine channel topology. *Neuropharmacology.* 35:797–804.

Imoto, K., C. Busch, B. Sakmann, M. Mishina, T. Konno, J. Nakai, H. Bujo, Y. Mori, K. Fukuda, and S. Numa. 1988. Rings of negatively charged amino acids determine the acetylcholine receptor channel conductance. *Nature.* 335:645–648.

Javitch, J.A., D. Fu, G. Liapakis, and J. Chen. 1997. Constitutive activation of the beta 2-adrenergic receptor alters the orientation of its sixth membrane-spanning segment. *J. Biol. Chem.* 272:18546–18549.

Karlin, A., and M.H. Akabas. 1998. Substituted-cysteine accessibility method. *Methods Enzymol.* 293:123–145.

Kienker, P.K., W.F. DeGrado, and J.D. Lear. 1994. A helical-dipole model describes the single-channel current rectification of an uncharged peptide ion channel. *Proc. Natl. Acad. Sci. USA.* 91: 4859–4863.

Kobilka, B.K., R.A. Dixon, T. Frielle, H.G. Dohlman, M.A. Bolanowski, I.S. Sigal, T.L. Yang-Feng, U. Francke, M.G. Caron, and R.J. Lefkowitz. 1987. cDNA for the human beta 2-adrenergic receptor: a protein with multiple membrane-spanning domains and encoded by a gene whose chromosomal location is shared with that of the receptor for platelet-derived growth factor. *Proc. Natl. Acad. Sci. USA.* 84:46–50.

Linsdell, P., and J.W. Hanrahan. 1996. Flickery block of single CFTR chloride channels by intracellular anions and osmolytes. *Am. J. Physiol.* 271:C628–C634.

Linsdell, P., J.A. Tabcharani, and J.W. Hanrahan. 1997. Multi-ion mechanism for ion permeation and block in the cystic fibrosis transmembrane conductance regulator chloride channel. *J. Gen. Physiol.* 110:365–377.

Linsdell, P., S.X. Zheng, and J.W. Hanrahan. 1998. Non-pore lining amino acid side chains influence anion selectivity of the human CFTR Cl^- channel expressed in mammalian cell lines. *J. Physiol.* 512:1–16.

Linsdell, P., A. Evagelidis, and J.W. Hanrahan. 2000. Molecular determinants of anion selectivity in the cystic fibrosis transmembrane conductance regulator chloride channel pore. *Biophys. J.* 78:2973–2982.

Liu, X., S.S. Smith, F. Sun, and D.C. Dawson. 2001. CFTR: Covalent modification of cysteine-substituted channels expressed in *Xenopus oocytes* shows that activation is due to the opening of channels resident in the plasma membrane. *J. Gen. Physiol.* 118:433–446.

Liu, Y., M.E. Jurman, and G. Yellen. 1996. Dynamic rearrangement of the outer mouth of a K^+ channel during gating. *Neuron.* 16: 859–867.

Lu, Z., and R. MacKinnon. 1994. Electrostatic tuning of Mg^{2+} affinity in an inward-rectifier K^+ channel. *Nature.* 371:243–246.

MacKinnon, R., R. Latorre, and C. Miller. 1989. Role of surface electrostatics in the operation of a high-conductance Ca^{2+}-activated K^+ channel. *Biochemistry.* 28:8092–8099.

MacKinnon, R., and C. Miller. 1989. Functional modification of a Ca^{2+}-activated K^+ channel by trimethyloxonium. *Biochemistry.* 28: 8087–8092.

Mansoura, M.K., S.S. Smith, A.D. Choi, N.W. Richards, T.V. Strong, M.L. Drumm, F.S. Collins, and D.C. Dawson. 1998. CFTR: Anion binding as a probe of the pore. *Biophys. J.* 74:1320–1332.

McCarty, N.A. 2000. Permeation through the CFTR chloride channel. *J. Exp. Biol.* 203:1947–1962.

McCarty, N.A., S. McDonough, B.N. Cohen, J.R. Riordan, N. Davidson, and H.A. Lester. 1993. Voltage-dependent block of the cystic fibrosis transmembrane conductance regulator Cl^- channel by two closely related arylaminobenzoates. *J. Gen. Physiol.* 102:1–23.

McCarty, N.A., and Z.-R. Zhang. 2001. Identification of a region of strong discrimination in the pore of CFTR. *Am J. Physiol.* In press.

McDonough, S., N. Davidson, H.A. Lester, and N.A. McCarty. 1994. Novel pore-lining residues in CFTR that govern permeation and open-channel block. *Neuron.* 13:623–634.

Overholt, J.L., M.E. Hobert, and R.D. Harvey. 1993. On the mechanism of rectification of the isoproterenol-activated chloride current in guinea-pig ventricular myocytes. *J. Gen. Physiol.* 102:871–895.

Overholt, J.L., A. Saulino, M.L. Drumm, and R.D. Harvey. 1995. Rectification of whole cell cystic fibrosis transmembrane conductance regulator chloride current. *Am. J. Physiol.* 268:C636–C646.

Pascual, J.M., C.C. Shieh, G.E. Kirsch, and A.M. Brown. 1995. K^+ pore structure revealed by reporter cysteines at inner and outer surfaces. *Neuron.* 14:1055–1063.

Riordan, J.R., J.M. Rommens, B. Kerem, N. Alon, R. Rozmahel, Z. Grzelczak, J. Zielenski, S. Lok, N. Plavsic, J.L. Chou, et al. 1989. Identification of the cystic fibrosis gene: cloning and characterization of complementary DNA [published erratum appears in *Science.* 1989. 245:1437]. *Science.* 245:1066–1073.

Sheppard, D.N., D.P. Rich, L.S. Ostedgaard, R.J. Gregory, A.E. Smith, and M.J. Welsh. 1993. Mutations in CFTR associated with mild-disease-form Cl^- channels with altered pore properties. *Nature.* 362:160–164.

Singh, R., G.V. Lamoureux, W.J. Lees, and G.M. Whitesides. 1995. Reagents for rapid reduction of disulfide bonds. *Methods Enzymol.* 251:167–173.

Smith, S. S., E.D. Steinle, M.E. Meyerhoff, and D.C. Dawson. 1999. Cystic fibrosis transmembrane conductance regulator. Physical basis for lyotropic anion selectivity patterns. *J. Gen. Physiol.* 114: 799–818.

Solomons, T.W.G., and C.B. Fryhle. 2000. Organic Chemistry. John Wiley & Sons, Inc., New York. 1089 pp.

Stryer, L. 1988. Biochemistry. W.H. Freeman and Company, New York. 1258 pp.

Tabcharani, J.A., J.M. Rommens, Y.X. Hou, X.B. Chang, L.C. Tsui, J.R. Riordan, and J.W. Hanrahan. 1993. Multi-ion pore behaviour in the CFTR chloride channel. *Nature.* 366:79–82.

Wilkinson, D.J., M.K. Mansoura, P.Y. Watson, L.S. Smit, F.S. Collins, and D.C. Dawson. 1996. CFTR: the nucleotide binding folds regulate the accessibility and stability of the activated state. *J. Gen. Physiol.* 107:103–119.

Yang, J., Y.N. Jan, and L.Y. Jan. 1995. Control of rectification and permeation by residues in two distinct domains in an inward rectifier K^+ channel. *Neuron.* 14:1047–1054.

Zhang, H.J., Y. Liu, R.D. Zuhlke, and R.H. Joho. 1996. Oxidation of an engineered pore cysteine locks a voltage-gated K^+ channel in a nonconducting state. *Biophys. J.* 71:3083–3090.

Zhang, Z.R., S.I. McDonough, and N.A. McCarty. 2000a. Interaction between permeation and gating in a putative pore domain mutant in the cystic fibrosis transmembrane conductance regulator. *Biophys. J.* 79:298–313.

Zhang, Z.R., S. Zeltwanger, and N.A. McCarty. 2000b. Direct comparison of NPPB and DPC as probes of CFTR expressed in Xenopus oocytes. *J. Membr. Biol.* 175:35–52.